Influence of Systematic Variations of Molecular Geometries of Small Hydrocarbons on *ab initio* HF/6-31G* and 6-311G* GIAO Calculated ^{1}H and ^{13}C NMR Chemical Shifts

Thomas Zuschneid and Guenter Haefelinger*

Institute of Organic Chemistry, University of Tuebingen, Auf der Morgenstelle 18, D-72076 Tuebingen, Germany

Abstract: GIAO HF calculations with symmetry retaining variations of selected CH or CC distances in a large range but constant retention of other geometric parameters have been performed for 10 molecules using the 6-31G* basis set (**set A**) and for a larger set of 18 molecules **1** to **18** in the 6-311G* basis set (**set B**). The graphical representations for calculated ^{1}H NMR shifts in dependence on CH or CC bond lengths variations are mostly linear or slightly curved and show no extreme values in the range studied. The slopes are generally positive, i. e. an elongation of distances leads to low field shifts because of reduction of the density of shielding electrons in the varied bonds. The slopes of regression lines may be classified for CH bonds according to hybridization and with the kind of substitution. Calculated ^{13}C NMR chemical shifts are dependent for connected C atoms on variations of CC as well as on CH bond distances. The graphs are mostly curved, also positive and in magnitude dependent on the types of bonds. Two dimensional plots of simultaneous variations of CH and CC bonds show for ^{1}H NMR independent behavior of these parameters. The effect of variations of angles on ^{1}H and ^{13}C shifts was studied only for a few molecules and shows curved graphs with rather small slopes. The determined slopes of linear regressions may be used to estimate zero-point vibrational corrections in close agreement to directly calculated values.

INTRODUCTION

Ab initio GIAO MO calculations of NMR chemical shieldings or of TMS based chemical shifts are useful tools for predictions of ^{1}H or ^{13}C NMR spectra as reviewed lately [1-3].

A basic problem for the calculation of magnetic properties is the selection of a gauge origin for the vector potential in the molecular electronic Hamiltonian which represents not uniquely the applied external magnetic field [4]. A first solution to this gauge problem was the use of individual gauges for localized molecular orbitals (IGLO) by the group of Kutzelnigg [5,6] and other approaches like LORG [7] or CSGT [8]. But the nowadays most widely used approach is termed GIAO from gauge including atomic orbitals. Such orbitals had been already suggested in 1937 by London for simple HMO calculations of magnetic susceptibilities [9]. Later, Ditchfield introduced them into ab initio Hartree-Fock (HF) theory [10,11] and since Pulay *et al.* [12] developed an efficient computer implementation in 1990, the GIAO method has become a standard for calculating NMR chemical shifts, installed in most quantum chemical ab initio programs like GAUSSIAN 98 [13] or GAUSSIAN 03 [14] which we used here.

To start a GIAO calculation, a molecular geometry has to be selected which may be taken from experiment or obtained by ab initio gradient optimization for the molecule in an appropriate basis set. Ab initio calculations of geometries usually refer to isolated rigid molecules with fixed conformations at 0 K and the GIAO calculations of shieldings are affected by the following aspects:

1. Selection of molecular geometries [15-17].

2. Extent and flexibility of basis sets [18-21].

3. Procedures of calculations (a comparison of the performance of HF, DFT and MP2 is presented in ref. [20]) with the following factors:

a) The single-determinantal self-consistent field Hartree-Fock (HF) method [22] serves as the traditional standard type approach [16,19,20].

b) This standard seems now to be replaced by density functional theory (DFT) [23] which incorporates in formulations for the exchange-correlation functional effects of electron correlation, but has some empirical character and total energies do not fulfill the quantum mechanical variation principle.

c) Post-Hartree-Fock methods: For very accurate calculations, post-HF methods leading to improved treatment of electron correlation are necessary as developed and reviewed lately by Gauss *et al.* [2]: One approach for this is the many-body perturbation theory by Møller and Plesset [24] with a perturbative treatment of higher excitations of second order as MP2 [25], third and forth order as MP3 and MP4 [26].

*Address correspondence to this author at the Institute of Organic Chemistry, University of Tuebingen, Auf der Morgenstelle 18, D-72076 Tuebingen, Germany; E-mail: guenter.haefelinger@uni-tuebingen.de

Table 1.   Molecules Studied and Indication of Variations of Parameters

No. of Molecules for	Molecule	Molecular Symmetry	Parameter	BO [a]	Variation in set A [b]			Optimized Distance [b,c] for set B
					Start	**End**	**Step**	
1	Methane	T_d	CH		1.0262	1.1492	0.003	1.0854
2	Ethane	D_{3d}	CH		1.0100	1.1677	0.01	1.0884
			CC	1	1.4280	1.6280	0.01	1.5230
			∡ CCH		106.55°	116.55°	0.5°	
3	Ethene	D_{2h}	CH		1.001	1.161	0.01	1.0804
			CC	2	1.234	1.434	0.01	1.3319
			∡ CCH		116.32	126.32	0.5°	
4	Ethyne	$D_{\infty h}$	CH		1.02	1.14	0.01	1.0614
			CC	3	1.10	1.29	0.01	1.2114
5	Propane	C_{2v}	C^1-H^i		1.0504	1.1304	0.005	1.0888
			C^1-H^o		1.0511	1.1311	0.005	1.0899
			C^2-H^2		1.0517	1.1317	0.005	1.0909
			C^1-C^2	1	1.4306	1.6306	0.02	1.5231
			∡ CCC		102.7678°	122.7678°	1°	
6	Butadiene	C_{2h}	C^1-H^c		1.00	1.16	0.01	1.0818
			C^1-H^t		1.00	1.16	0.01	1.0799
			C^2-H^2		1.00	1.16	0.01	1.0845
			C^1-C^2	2	1.34	1.62	0.02	1.3400
			C^2-C^3	1	1.20	1.46	0.02	1.4536
7	Benzene	D_{6h}	CH		1.00	1.16	0.01	1.0815
			CC	1,5	1.26	1.52	0.02	1.3936
8	Cyclopropane	D_{3h}	CH					1.0784
			CC	1				1.5040
9	Propene	C_s	C^1-H^c		1.01	1.14	0.01	1.0821
			C^1-H^t		1.01	1.14	0.01	1.0803
			C^2-H^2		1.01	1.14	0.01	1.0845
			C^3-H^i					1.0884
			C^3-H^o					1.0902
			C^1-C^2	2	1.24	1.42	0.01	1.3335
			C^2-C^3	1	1.44	1.62	0.01	1.4954
10	Allene	D_{2d}	C^1-H					1.0808
			C^1-C^2	2				1.3082
11	Propyne	C_{3v}	C^1-H^1		1.01	1.14	0.01	1.0607
			C^3-H^3		1.01	1.14	0.01	1.0881
			C^1-C^2	3	1.00	1.40	0.01	1.2138
			C^2-C^3	1	1.40	1.70	0.01	1.4588

(Table 1). Contd…..

No. of Molecules for	Molecule	Molecular Symmetry	Parameter	BO [a]	Variation in set A [b]			Optimized Distance [b,c] for set B
					Start	End	Step	
12	Butane	C_{2h}	C^1-H^i					1.0893
			C^1-H^o					1.0897
			C^2-H^2					1.0915
			C^1-C^2	1				1.5224
			C^2-C^3	1				1.5306
13	Isobutane	C_{3v}	C^1-H^i					1.0912
			C^1-H^o					1.0900
			C^2-H^2					1.0929
			C^1-C^2	1				1.5239
14	Butene	C_{2h}	C^1-H^i					1.0886
			C^1-H^o					1.0905
			C^2-H^2					1.0859
			C^1-C^2	1				1.4955
			C^2-C^3	2				1.3355
15	Isobutene	C_{2v}	C^1-H^1		1.01	1.14	0.01	1.0811
			C^3-H^i		1.01	1.14	0.01	1.0877
			C^3-H^o		1.01	1.14	0.01	1.0914
			C^1-C^2	2	1.44	1.62	0.01	1.3365
			C^2-C^3	1	1.24	1.42	0.01	1.4995
16	Butyne	D_{3h}	C^1-H					1.0887
			C^1-C^2	1				1.4594
			C^2-C^3	3				1.2157
17	Butadiyne	$D_{\infty h}$	C^1-H					1.0619
			C^1-C^2	3				1.2194
			C^2-C^3	1				1.3687
18	Neopentane	T_d	C^1-H					1.0909
			C^1-C^2	1				1.5264
19	TMS	T_d	CH					1.0902
			SiC					1.8826

[a]Formal CC bond order. [b]Distances in Å, angles in °. [c]Distances obtained by MP2/cc-pVTZ optimizations are kept constant if not varied.

As most advanced treatment of electron correlation, the coupled cluster (CC) theory has been introduced for single and double excitations (CCSD) [27,28] and perturbative corrected triple excitations (CCSD(T)) [29]. In multi-configuration SCF theory (MCSCF) [30], a linear combination of several Slater determinants is used.

1. Rovibrational and thermal effects [31-34] take care about the thermal occupation of rotational and vibrational levels from 0 K to the experimental measuring conditions around 300 K. These are not routinely calculated and available only lately, but necessary for accurate predictions of absolute shieldings.

2. Relativistic effects [35] are important for heavy atoms but not for the hydrocarbons studied here.

3. Environmental effects [36] have to be considered if solution NMR spectra are used for comparison, as well as a pressure dependence [37,38] for gas phase data.

4. For determinations of chemical shifts the NMR shielding of the standard TMS has to be calculated in a selected geometry (an experimental electron diffraction (ED) r_g structure was reported recently [39]), usually in the same basis set as that of the considered molecule.

Most papers on GIAO NMR calculations concentrate on shieldings of ^{13}C and various heteroatom nuclei and only a few on ^{1}H spectra [18,21,40-42].

Benchmark type calculations for non-hydrogen NMR shieldings of small molecules using most advanced CI methods like CCSD(T) [28] and CCSDT [43] with large basis sets lead to agreements in the range of experimental accuracy. However, this level of precision cannot be extended to larger systems and with less advanced procedures deviations in the range of ± 5 ppm are obtained for ^{13}C and ± 1 ppm for [1]H.

GIAO calculations based on a geometry optimized in the same or an other basis set implicitly contain a contribution due to basis set dependent changes in molecular geometry.

To eliminate this effect we studied lately [44] the dependence of GIAO calculated ^{1}H and ^{13}C NMR shieldings and chemical shifts of seven hydrocarbons on different standard basis sets, independent on variations of the underlying molecular geometry, for which purpose we selected experimental r_e distances (referring to global minima on the energy hypersurface). We used 25 basis sets for the HF level of theory, 16 basis sets for the hybrid DFT method B3LYP (Becke´s three-parameter functional with exact HF exchange

and Lee-Yang-Parr exchange-correlation) [45,46], and 12 basis sets for the MP2 approach. For experimental ^{13}C values independent of solvation effects we used the gas phase data of ref. [38] (which are extrapolated to zero pressure) and own determinations of gas phase ^{1}H chemical shifts at atmospheric pressure [44].

The performance of each basis set based on accurate experimental r_e distances in relation to experimental gas phase NMR shifts was quantified by means of statistical linear least squares regressions considering the quality by mean deviations, correlation coefficients, standard deviations and the slopes of the best fit straight lines. Useful precisions may be obtained already by using Pople´s standard 6-31G* and 6-311G* basis sets in the HF procedure.

Much less is known on the influence of systematic variations of selected bond distances or angles on GIAO calculated NMR shifts which is the aim of this study. What is an "exact" geometry for GIAO calculations? Are preferred distances observable? Is the shape of dependences on varied CH or CC distances linear with positive or negative slopes, or curved in a concave or convex manner, or are minima or maxima observable within the studied range?
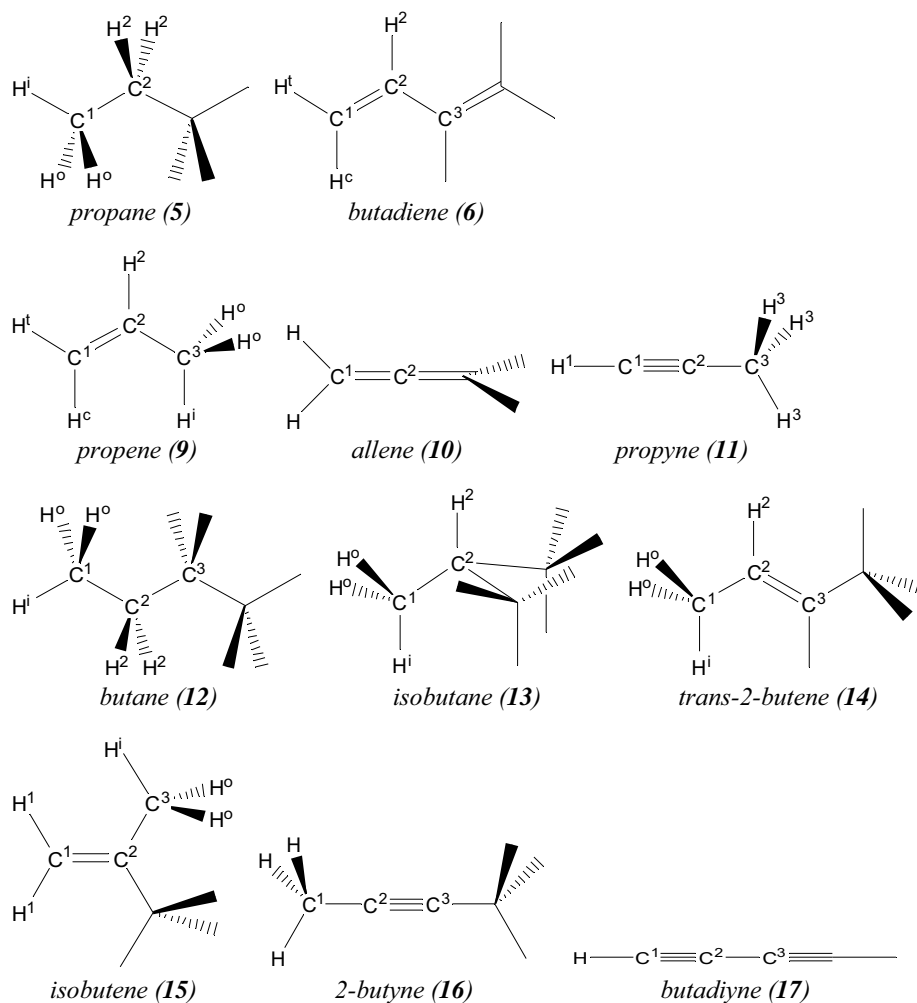
Fig. (1). Structural formulas of molecules **5, 6, a**nd **9-17**. Numbered are only atoms used in the variations. Not designated are symmetry equivalent atoms, except C[3] of C4 chains, which are necessary to name the central CC bonds.

a   **b**
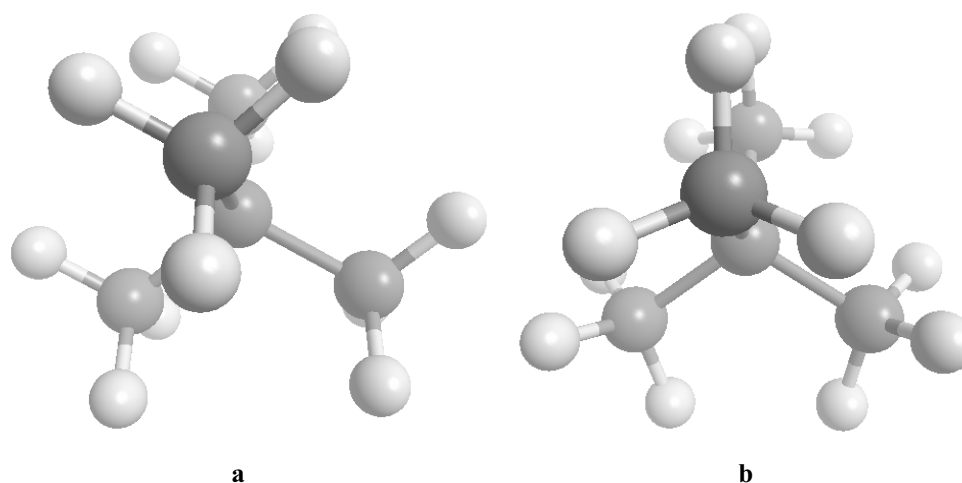
Fig. (2). Left the staggered (**a**), right the ecliptic geometry (**b**) of neopentane (**18**) and TMS (**19**). Both are of T_d symmetry, but only the staggered form **a** is the minimum.

DETAILS OF CALCULATIONS

Selection of Molecules and Basis Sets

All hydrocarbons **1** to **18** which are studied here are listed in Table **1** and necessary numbering of atoms is shown in Fig. (**1**). A first **set A** contains 10 molecules **1** to **7** (which had been considered for basis set dependences in ref. [44]) and additionally **9**, **11** and **15**. A second **set B** contains the molecules **1** to **18** which represent all main types of CC bonding (single, double and triple bonds as well as sp^3, sp^2 and sp hybridizations of carbon) and all types of carbon (primary to quaternary) in hydrocarbons. The variation of the geometry of the molecules of **set A** was studied by HF calculations in Pople´s 6-31G* basis set of double zeta quality and those of **set B** in the 6-311G* basis set of triple zeta quality, both with polarization d-functions on carbon. The shieldings of TMS which are needed for conversion to chemical shift values have been derived for a T_d geometry optimized in these two basis sets leading to the following NMR values: from HF/6-31G* calculations 32.9035 ppm for ^{1}H and 201.7285 ppm for ^{13}C, and from HF/6-311G* calculations 32.8505 ppm for ^{1}H and 195.9890 ppm for [13]C.

Variations of Molecular Geometries

For each considered molecule, the internal coordinate of one typical parameter (a bond length or a CCH angle) was varied in a selected range in defined steps while retaining the molecular symmetry (which is indicated in Table **1**) and keeping all other parameters constant, i. e. for methane (**1**) all four CH distances or for staggered ethane (**2**) all six CH distances are varied simultaneously. Alkyl group conformations are taken mostly as staggered, except for isobutene (**15**) and 2-butyne (**16**) with minimum conformations as shown in Fig. (**1**). For neopentane (**18**) and TMS (**19**), two conformations of T_d symmetry are possible which are shown in Fig. (**2**), but only the staggered forms **18a** and **19a** represent minima. Generally, dihedral angles have not been varied but kept constant.

For molecules **1** to **7** of **set A**, the r_e geometries of ref. [44] and for **9**, **11** and **15** HF/6-31G* optimized values were

used as starting geometries for those parameters which have to be kept constant. Step sizes, minima and maxima of the varied parameters are presented in Table **1**. For each step of the distance variation, a HF/6-31G* GIAO calculation was performed. The derived absolute shieldings were converted to NMR chemical shifts (δ) by use of the before mentioned TMS shieldings.

Molecules **1** to **18** of the **set B** were treated differently: Starting geometries were determined for each molecule by MP2 optimizations [24] using the correlation consistent polarized valence triple zeta cc-pVTZ basis set of Dunning [47] with resulting distances listed in Table **1**, which approximate r_e distances with high reliability [48]. The status of obtained conformations as minima were confirmed by frequency calculations. Varied parameters were classified according to types of bonds with starting and final values and the step sizes as given in Table **2**.

Table 2. Ranges of Variations and Step Sizes (in Å) for the 6-311G* Calculations of Set B

Parameter	Start	End	Step
CH	1.00	1.16	0.01
CC single	1.40	1.66	0.02
C=C double	1.20	1.46	0.02
C≡C triple	1.06	1.34	0.02
CC butadiene central	1.34	1.62	0.02
CC butadiyne central	1.24	1.50	0.02
CC benzene	1.26	1.52	0.02
SiC TMS	1.73	2.05	0.02

Each distance variation was evaluated by linear or polynomial regressions and will be presented only in tables or in graphical form.

RESULTS AND DISCUSSIONS

Dependences of ^{1}H NMR Shifts on Variations of CH-Distances

It is quite expectable that ^{1}H NMR chemical shifts will be very dependent on the changes of CH distances between the selected proton and the connected carbon atom. The distance dependence of the chemical shifts of hydrogens bonded to sp^2 hybridized carbons for **set A** leads to graphs which are perfectly linear or close to linearity with a slightly concave curvature and they are nearly parallel.

Table 3. Linear Regressions of ^{1}H Shifts Versus CH Distances. n_{hyb} Denotes the p-part of Hybridization of the Involved Carbon Atom, e. g. 1 for sp, 2 for sp^2, and 3 for sp^3. n_{ox} is the Oxidation Number and n_{CH} the Number of Simultaneously Varied CH Distances Per Carbon

No. of molecules	Varied Distance	n_{hyb}	n_{ox}	n_{CH}	Set A			Set B		
					m	R^2	Type [a]	m	R^2	Type [a]
1	H-C	3	-4	4	33.7024	0.9987	A	34.9722	0.9973	M
2	H-C	3	-3	3	33.0841	0.9977	A	34.5370	0.9974	M
3	H-C	2	-2	2	17.2058	0.9995	L	17.7030	0.9994	L
4	H-C	1	-1	1	31.7770	0.9989	A	32.3126	0.9980	A
5	H^i-C^1	3	-3	1	24.0650	0.9994	L	25.1468	0.9974	M
5	H^o-C^1	3	-3	2	27.4242	0.9995	L	28.7666	0.9975	M
5	H^2-C^2	3	-2	2	26.8276	0.9994	L	28.3239	0.9972	M
6	H^c-C^1	2	-2	1	16.5980	0.9987	A	16.7507	0.9985	A
6	H^t-C^1	2	-2	1	16.8268	0.9988	A	17.0519	0.9986	A
6	H^2-C^2	2	-1	1	14.9660	0.9989	A	14.6642	0.9989	A
7	H-C	2	-1	1	13.3867	0.9994	L	13.3028	0.9994	L
8	H-C	3	-2	2				33.5332	0.9980	A
9	H^c-C^1	2	-2	1	17.0182	0.9991	L	16.8140	0.9984	A
9	H^t-C^1	2	-2	1	17.2718	0.9991	L	17.1395	0.9985	A
9	H^2-C^2	2	-1	1	15.1315	0.9992	L	14.6363	0.9987	A
9	H^i-C^3	3	-3	2				24.6864	0.9974	M
9	H^o-C^3	3	-3	1				27.8402	0.9975	M
10	H-C	2	-2	2				22.4967	0.9984	A
11	H^1-C^1	1	-1	1	31.0584	0.9987	A	30.7929	0.9981	A
11	H^3-C^3	3	-3	3	31.7030	0.9984	A	31.9546	0.9974	M
12	H^i-C^1	3	-3	1				25.1151	0.9974	M
12	H^o-C^1	3	-3	2				28.3430	0.9974	M
12	H^2-C^2	3	-2	2				29.2450	0.9974	M
13	H^i-C^1	3	-3	1				24.6618	0.9976	M
13	H^o-C^1	3	-3	2				28.3556	0.9977	M
13	H^2-C^2	3	-1	1				23.9257	0.9970	M
14	H^i-C^1	3	-3	1				24.6296	0.9974	M
14	H^o-C^1	3	-3	2				28.0118	0.9976	M
14	H^2-C^2	2	-1	1				15.4212	0.9988	A
15	H^1-C^1	2	-2	2	18.8693	0.9993	L	19.2649	0.9987	A
15	H^i-C^3	3	-3	1	25.5276	0.9987	A	24.8461	0.9975	M
15	H^o-C^3	3	-3	2	27.4492	0.9986	A	27.7956	0.9976	M
16	H-C	3	-3	3				32.0344	0.9974	M
17	H-C	1	-1	1				32.1993	0.9981	A
18	H-C	3	-3	3				32.2789	0.9975	M
19	H-C	3	-3	3				33.4250	0.9975	M

[a] L = highly linear, A = approximately linear, M = only moderate linear fit.
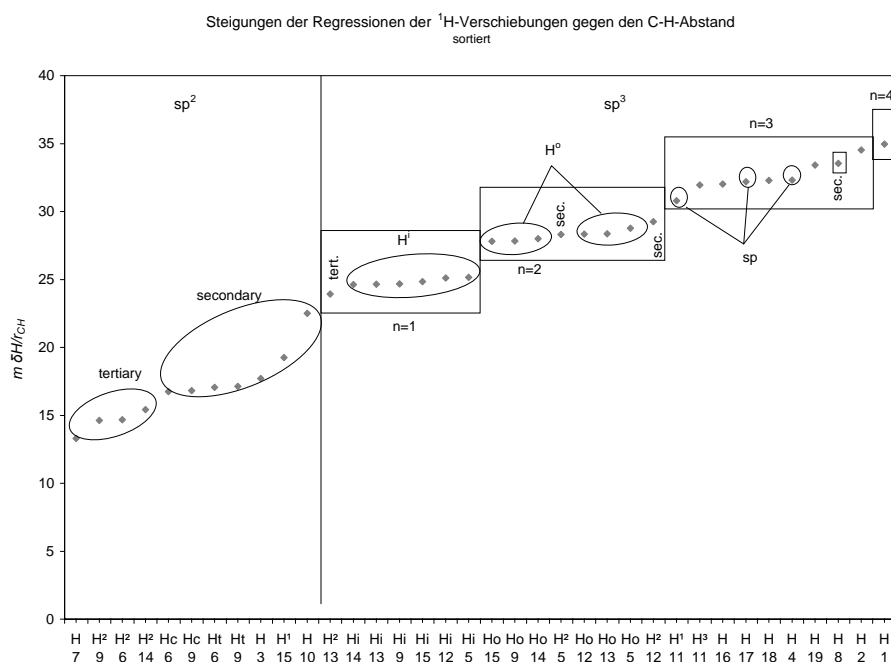
Fig. (3). Slopes (m) of the linear regressions of ¹H shifts versus the CH distance, plotted in ascending order for all molecules of **set B**. (Bottom line is numbering of molecules).

Table **3** presents the slopes (*m*) and coefficients of determination (R^2) as measures of certainty for linear correlations of shifts with CH distances for all molecules of both sets (**A** and **B**). There are no maxima or minima observable within the range of variations. (This holds even in the case of methane (**1**) tested for an extreme range from 0.1 to 2.0 Å which is physically meaningless.) The values of R^2 in Table **3** are all between 0.9973 to 0.9995, indicating a high statistical relevance. But only cases with R^2 larger than 0.999 are considered as strictly linear. This holds for molecules **3**, **5**, **7** and **9** of set **A** and only **3** and **7** of set **B**. The slopes of set **B** are in a similar range as those of set **A**, i. e. the dependence of geometry variations seems to be independent on the kind of applied basis set. A slight curvature is more often found in set **B** than in set **A**.

All slopes *m* of linear regressions for the varied distances of set **B** are plotted in Fig. (**3**) in ascending order. This leads to the following classification as indicated in the graph: Hydrogens connected to sp^2 carbons show smallest slopes and may be grouped in tertiary and secondary CH bonds. Hydrogen atoms at saturated sp^3 hybridized carbon atoms lead to larger slopes which may be classified into three classes according to the number (n_{CH}) of varied CH bonds at the considered carbon atom. The tertiary CH bond of **13** with $n_{CH} = 1$ is in the same class as the primary in-plane CH^i bonds of **5**, **9**, and **12** to **15**, whereas corresponding out-of-plane CH^o bonds with $n_{CH} = 2$ form a class together with the secondary CH^2 bonds of propane (**5**) and butane (**12**). However, the secondary CH^2 groups of cyclopropane (**8**) are not found there, but in the class for $n_{CH} = 3$ together with the slopes for sp CH bonds. The slope of methane (**1**) indicates the largest distance dependence of all studied variations.

The observed uniformly positive slope with enlargement of distances corresponds to a low field shift in the NMR spectrum which may be interpreted by a reduction of elec-

tron densities at hydrogen. This effect may be enhanced with the number n_{CH} of simultaneously varied bonds as observed for the classes in Fig. (**3**).

Dependences of ¹³C NMR Shifts on Variations of CH Distances

¹³C shifts also are strongly dependent on variations of CH bond lengths to the considered carbon atom. Regression lines for variations of sp^3 CH bonds of set **A** are again linear or close to linearity, now with a slightly convex deviation, but show groups of different slopes *m*. These are collected numerically in Table **4** for all varied distances. They span a large range from 6.1 to 203.4 ppm. R^2 values indicate high reliability and are all larger than 0.99. Again, only those larger than 0.999 are considered as strictly linear.

Linear and polynomial regressions for the larger set **B** are shown in Table **5**. Linearity is obtained only for some sp^3 hybridized CH bonds in seven molecules. The bond length variations for ¹³C shifts may be treated successfully by quadratic regressions leading to very high R^2 values and standard deviations (s_{quad}) generally much less than 0.015 ppm, in contrast to those of linear regressions (s_{lin}).

The quadratic regression uses the second order polynomial (eqn. 1) for the least squares approximation of data points. Its second derivative is here termed curvature (*c*) as defined in eq n. 2.

$$f(x) = a_2 x^2 + a_1 x + a_0 \tag{1}$$

$$c = f''(x) = 2a_2 \tag{2}$$

The values in Table **5** are classified by the kind of hybridization sp^n with $n_{hyb} = 1$, 2 or 3, the oxidation numbers of carbon (n_{ox}) and the numbers of varied CH bonds (n_{CH}). Linear slopes (*m*) for saturated carbons ($n_{hyb} = 3$), averaged in the groups of $n_{CH} = 1$, 2, 3 are approximately close to a ratio

Table 4.   Linear Regressions of ¹³C Shifts Versus CH Distances of Set A

No.	Group	n_{hyb}	n_{CH}	m	R^2	Type [a]
1	C-H	3	4	201.5270	0.9999	L
2	C-H	3	3	203.4425	0.9998	L
3	C-H	2	2	57.7253	0.9960	M
4	C-H	1	1	6.1344	0.9861	M
5	C^1-H^i	3	1	54.0162	0.9994	L
5	C^1-H^o	3	2	129.0827	0.9998	L
5	C^2-H^2	3	2	139.1451	0.9998	L
6	C^1-H^c	2	1	37.6980	0.9947	M
6	C^1-H^t	2	1	37.6388	0.9940	M
6	C^2-H^2	2	1	37.5468	0.9962	M
7	C-H	2	1	36.7760	0.9952	M
9	C^1-H^c	2	1	34.5453	0.9959	M
9	C^1-H^t	2	1	32.1744	0.9954	M
9	C^2-H^2	2	1	8.9747	0.9948	M
11	C^1-H^1	1	1	18.4007	0.9915	M
11	C^3-H^3	3	3	140.8375	0.9997	L
15	C^1-H^1	2	2	71.4980	0.9975	M
15	C^3-H^i	3	1	70.6905	0.9985	A
15	C^3-H^o	3	2	94.4754	0.9989	A

[a]See footnote to Table 3.

Table 5.   Linear and Polynomial Regressions of the ¹³C Shifts of set B Versus CH Distances, Ordered by p-part of Hybridization (n_{hyb}), Oxidation Number (n_{ox}), and Number of CH Bonds (n_{CH})

No.	Group	n_{hyb}	n_{ox}	n_{CH}	m	s_{lin} [a]	R^2_{lin}	[b]	c [c]	s_{quad} [d]	R^2_{quad}
4	C-H	1	-1	1	2.8586	0.0931	0.7193		81.9293	0.0015	0.9999303
11	C^1-H^1	1	-1	1	14.4575	0.1492	0.9623		131.2841	0.0004	0.9999998
17	C^1-H	1	-1	1	19.0334	0.1499	0.9777		131.8529	0.0003	0.9999999
6	C^2-H^2	2	-1	1	38.7320	0.1524	0.9943		134.0604	0.0031	0.9999978
7	C-H	2	-1	1	39.2631	0.1688	0.9933		148.4229	0.0052	0.9999940
9	C^2-H^2	2	-1	1	40.2408	0.1843	0.9923		162.1674	0.0024	0.9999988
14	C^2-H^2	2	-1	1	34.1409	0.1808	0.9898		159.0898	0.0024	0.9999984
6	C^1-H^c	2	-2	1	38.8170	0.1820	0.9920		160.0658	0.0021	0.9999990
6	C^1-H^t	2	-2	1	38.2298	0.1930	0.9907		169.8109	0.0020	0.9999991
9	C^1-H^c	2	-2	1	35.6193	0.1789	0.9908		157.3555	0.0020	0.9999990
9	C^1-H^t	2	-2	1	32.3105	0.1769	0.9891		155.6189	0.0020	0.9999987
3	C-H	2	-2	2	59.0580	0.2555	0.9932		224.7441	0.0045	0.9999981

(Table 5). Contd…..

No.	Group	n_{hyb}	n_{ox}	n_{CH}	m	s_{lin} [a]	R^2_{lin}	[b]	c [c]	s_{quad} [d]	R^2_{quad}
10	C^1-H	2	-2	2	82.0674	0.3076	0.9949		157.3555	0.0020	0.9999990
15	C^1-H^1	2	-2	2	70.1411	0.2837	0.9940		249.6311	0.0011	0.9999999
13	C^2-H^2	3	**-1**	1	82.9455	0.2046	0.9978		179.9866	0.0008	1.0000000
5	C^1-H^i	3	-3	1	53.3202	0.1636	0.9965		143.9466	0.0013	0.9999998
9	C^3-H^o	3	-3	1	101.7970	0.2391	0.9980	A	210.3212	0.0003	1.0000000
12	C^1-H^i	3	-3	1	53.9758	0.1762	0.9961		154.9807	0.0011	0.9999999
13	C^1-H^i	3	-3	1	69.4184	0.1729	0.9977		152.0658	0.0024	0.9999996
14	C^1-H^i	3	-3	1	58.6700	0.1704	0.9969		149.9252	0.0012	0.9999999
15	C^3-H^i	3	-3	1	52.7779	0.1600	0.9966		140.7990	0.0015	0.9999997
5	C^2-H^2	3	-2	2	143.9494	0.2734	0.9987	A	240.5423	0.0006	1.0000000
8	C-H	3	-2	2	149.5560	0.3693	0.9978		324.9358	0.0007	1.0000000
12	C^2-H^2	3	-2	2	167.4315	0.2504	0.9992	L	220.2405	0.0036	0.9999998
5	C^1-H^o	3	-3	2	131.8589	0.2555	0.9986	A	224.7699	0.0006	1.0000000
9	C^3-H^i	3	-3	2	59.5126	0.1691	0.9970		148.7301	0.0013	0.9999998
12	C^1-H^o	3	-3	2	122.4479	0.2601	0.9983	A	228.8377	0.0005	1.0000000
13	C^1-H^o	3	-3	2	117.0909	0.2204	0.9987	A	193.9342	0.0012	1.0000000
14	C^1-H^o	3	-3	2	102.3905	0.2412	0.9980	A	212.2054	0.0006	1.0000000
15	C^3-H^o	3	-3	2	108.2765	0.2419	0.9982	A	212.7902	0.0011	1.0000000
2	C-H	3	-3	3	213.2241	0.2109	0.9996	L	185.5583	0.0004	1.0000000
11	C^3-H^3	3	-3	3	142.1266	0.2147	0.9992	L	188.8060	0.0047	0.9999996
16	C^1-H	3	-3	3	144.9198	0.2074	0.9992	L	182.3973	0.0038	0.9999998
18	C^1-H	3	-3	3	62.4638	0.0343	0.9999	L	142.7361	0.0036	0.9999999
19	C-H	3	-3	3	176.8051	0.2426	0.9993	L	213.3612	0.0042	0.9999998
1	C-H	3	*-4*	*4*	201.0893	0.1660	0.9997	L	145.5475	0.0146	0.9999982

[a] Standard deviation of linear regression (esd). [b] Type of graph: L = linear, A = approximately linear. [c] Curvature (second derivative) of mixed quadratic regression. [d] esd of mixed quadratic regression.

of 1 : 2 : 3 (with exceptions for **9** and **18**), i. e. proportional to n_{CH}.

^{13}C shift variations for sp^2 CH bonds of **set B** are recognizably convex, indicated in Table **5** by lower linearity values (R^2_{lin}) around 0.99. The positive slopes m are again proportional to n_{CH} with slopes for **3**, **10** and **15** about twice as large as for the other sp^2 bonds. Of the sp systems, ethyne (**4**) shows a very low CH distance dependence of its ^{13}C shift. Its quadratic behavior is detectable in the enlarged scale of Fig. (**4**) in comparison to the larger distance dependence of propyne (**11**) and butadiyne (**17**). The numerical curvature values (c) of Table **5** allow no systematic interpretation.

Dependence of ^{1}H NMR Shifts on CC Distance Variations

The variation of CC distances leads to more structurally different situations as in the case of CH alternations. Fig. (**5**) shows the CC distance dependences of ^{1}H NMR shifts of some examples for CC single, double and triple bonds from **set A**. Only the sp triple bonds lead to linear graphs. The sp^2 double bond variations are very well represented by quadratic regressions. These are less accurate for sp^3 single bonds which show a small distance dependence with positive or even negative trends of slopes.
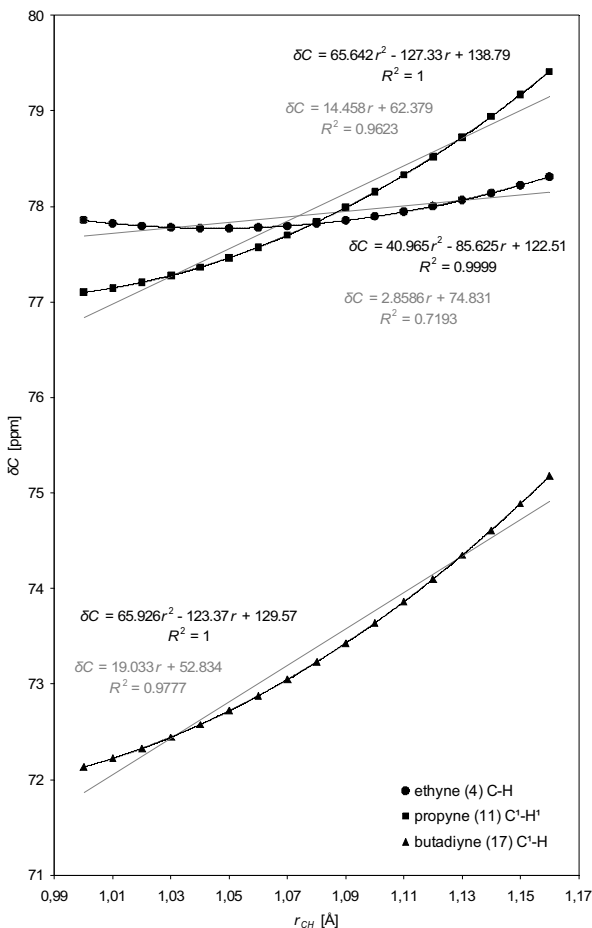
Fig. (4). ^{13}C shifts of sp hybridized carbon atoms of **set B** in dependence of CH distances with best linear and curved approximations and their equations.

Regression results for all compounds of **set B** are presented in Table **6** in the sequence of increasing bond order
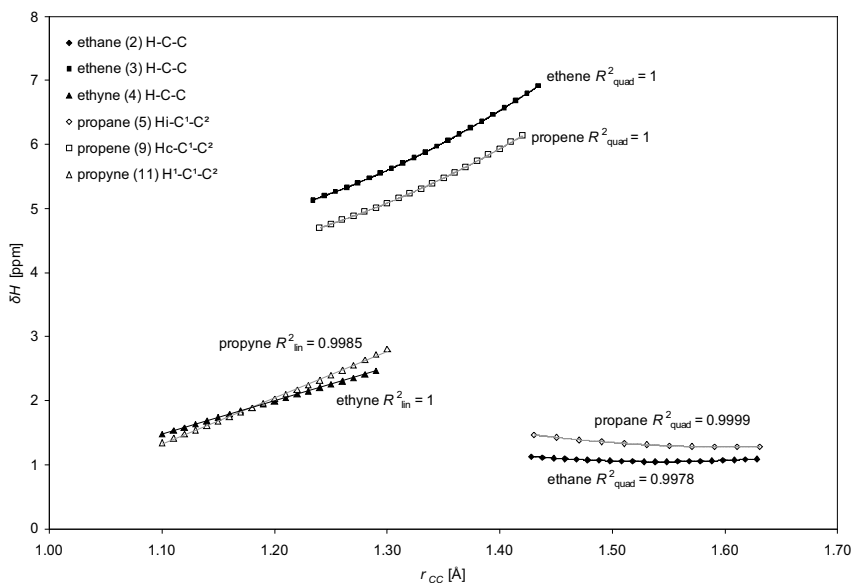
(BO). Here, approximations with polynomials up to fourth order according to eqn. 3 are reported, where each of the coefficients a_1 to a_4 may be zero.

$$f(x) = a_4 x^4 + a_3 x^3 + a_2 x^2 + a_1 x + a_0 \qquad (3)$$

The kind of non-zero coefficients is indicated in Table **6** by curly braces, i. e. {40} stands for a purely fourth order polynomial, {3210} for a mixed third order polynomial, {210} for the mixed quadratic polynomial (eqn. 1) and {10} for the linear regression. The best kind of representation is listed in the last column and best R^2 values are marked in gray.

Linearity with R^2 larger than 0.999 is only observed for the variation of the sp triple CC bonds in **4**, **17** and approximatively **11**. The effects of variations of sp^2 CC double bonds are mostly better approximated by the {40} polynomial than by the mixed quadratic polynomial {210}. The situation for sp^3 CC single bonds (BO = 1) is complex: mostly {210}, less often {3210} or even {40} may be best.

Fig. (**6**) shows nearly parallel descending curves for the effect of CC distance variation for in-plane CH^i bonds on ^{1}H shifts, except one ascending curve of isobutane (**13**), where the three equatorial CH^i bonds may be affected sterically by the variation of the CC bond.

Dependence of ^{13}C NMR Shifts on Variations of CC Distances

The distance variation of CC bonds is, as expectable, strongly affecting corresponding ^{13}C NMR shifts. For examples of **set B**, Fig. (**7**) clearly shows the influence of coordination of the considered sp^3 carbon atoms on the CC distance dependence of ^{13}C shifts: A largest linear effect for the quaternary C in neopentane (**18**), with positive slopes and nonlinearity decreasing with CC bond enlargements in the sequence of tertiary C in **13**, secondary C in **5** and primary C in **2**. The slopes of linear regressions decrease in an approximate ratio of 24 : 12 : 5 : 1. As in the case of ^{1}H shifts, the enlargement of CC bonds leads to a low-field NMR shift paralleling a dilution of bonding electron density.

Fig. (5). ^{1}H shifts of some compounds of **set A** with single, double, and triple bonds in dependence of CC distances.

Table 6. Linear ({10}), Mixed Quadratic ({210}), Fourth Order ({40}) and Mixed Cubic ({3210}) Regressions of ^{1}H Shifts (a) of Set B Versus CC Distances (b), Ordered by Bond Order (BO), Hybridization (n_{hyb}) and Oxidation Number (n_{ox})

	Group					{10}		{210}		{40}	{3210}	Best
No.	a	b	BO	n_{hyb}	n_{ox}	m	R^2	c	R^2	R^2	R^2	Type
6	H^2	C^2-C^3	1	2	-1	0.3131	0.8166	3.8642	0.99996	0.87246		{210}
9	H^2	C^2-C^3	1	2	-1	0.4523	0.8468	5.3719	0.99976	0.89346		{210}
14	H^2	C^2-C^1	1	2	-1	0.9286	0.9900	2.5992	0.99995	0.99901		{40}
13	H^2	C^2-C^1	1	3	-1	4.9385	0.9836	17.7912	0.99993	0.99649		{210}
5	H^2	C^2-C^1	1	3	-2	1.7149	0.9068	15.3434	0.99969	0.94312		{210}
8	H	C-C	1	3	-2	2.5823	0.9786	10.6350	0.99988	0.99398		{210}
12	H^2	C^2-C^1	1	3	-2	1.1352	0.7954	16.0525	0.99896	0.84835	0.999999	{3210}
12	H^2	C^2-C^3	1	3	-2	0.9997	0.8941	9.5896	0.99937	0.93280		{210}
2	H	C-C	1	3	-3	-0.3483	0.3960	11.9955	0.99709	0.32927	0.999994	{3210}
5	H^i	C^1-C^2	1	3	-3	-0.9086	0.8125	12.1875	0.99969	0.75533		{210}
5	H^o	C^1-C^2	1	3	-3	0.6361	0.7963	8.9797	0.99946	0.84928		{210}
9	H^i	C^3-C^2	1	3	-3	-0.6578	0.7146	11.6030	0.99920	0.64985		{210}
9	H^o	C^3-C^2	1	3	-3	-0.1133	0.0676	11.7387	0.99543	0.03698	0.999993	{3210}
11	H^3	C^3-C^2	1	3	-3	1.5609	0.8945	14.9609	0.99968	0.93325		{210}
12	H^i	C^1-C^2	1	3	-3	-0.4887	0.6580	9.8249	0.99833	0.59073	0.999993	{3210}
12	H^o	C^1-C^2	1	3	-3	-0.2207	0.2459	10.7682	0.99544	0.18878	0.999985	{3210}
13	H^i	C^1-C^2	1	3	-3	2.3366	0.9950	4.6439	0.99999	0.99997		{40}
13	H^o	C^1-C^2	1	3	-3	0.2415	0.2415	8.7349	0.99981	0.44225		{210}
14	H^i	C^1-C^2	1	3	-3	-0.5942	0.6774	11.4451	0.99919	0.61087		{210}
14	H^o	C^1-C^2	1	3	-3	0.2785	0.3083	11.6267	0.99605	0.37401	0.999990	{3210}
15	H^i	C^3-C^2	1	3	-3	-1.1456	0.8836	11.6202	0.99995	0.83527		{210}
15	H^o	C^3-C^2	1	3	-3	0.5541	0.6953	10.2349	0.99895	0.75721	0.999999	{3210}
16	H	C^1-C^2	1	3	-3	1.4330	0.8758	15.0491	0.99947	0.91785		{210}
18	H	C^1-C^2	1	3	-3	1.2887	0.9386	9.1937	0.99979	0.96764		{210}
7	H	C-C	1,5	2	-1	12.1317	0.9872	38.5213	0.99998	0.99867		{210}
6	H^2	C^2-C^1	2	2	-1	10.2941	0.9958	18.6195	1.00000	0.99975		{40}
9	H^2	C^2-C^1	2	2	-1	9.3230	0.9900	26.1473	0.99999	0.99960		{40}
14	H^2	C^2-C^3	2	2	-1	8.5071	0.9891	24.9241	0.99998	0.99941		{40}
3	H	C-C	2	2	-2	8.8957	0.9883	27.0690	0.99998	0.99920		{40}
6	H^c	C^1-C^2	2	2	-2	7.2669	0.9939	15.9021	1.00000	0.99999		{40}
6	H^t	C^1-C^2	2	2	-2	7.4626	0.9931	17.3723	1.00000	0.99999		{40}
9	H^c	C^1-C^2	2	2	-2	8.0778	0.9876	25.2641	0.99998	0.99902		{40}
9	H^t	C^1-C^2	2	2	-2	7.8292	0.9854	26.6377	0.99998	0.99832		{210}
10	H	C^1-C^2	2	2	-2	8.3617	0.9914	21.6442	0.99994	0.99983		{40}
15	H^1	C^1-C^2	2	2	-2	7.0780	0.9841	25.1477	0.99997	0.99785		{210}
4	H	C-C	3	1	-1	5.9735	0.9999	-1.1904	0.99999	0.98950		{10}
11	H^1	C^1-C^2	3	1	-1	7.9404	0.9970	11.0204	0.99980	0.99815		{210}
17	H	C^1-C^2	3	1	-1	6.0965	0.9999	-1.1679	0.99999	0.98952		{10}
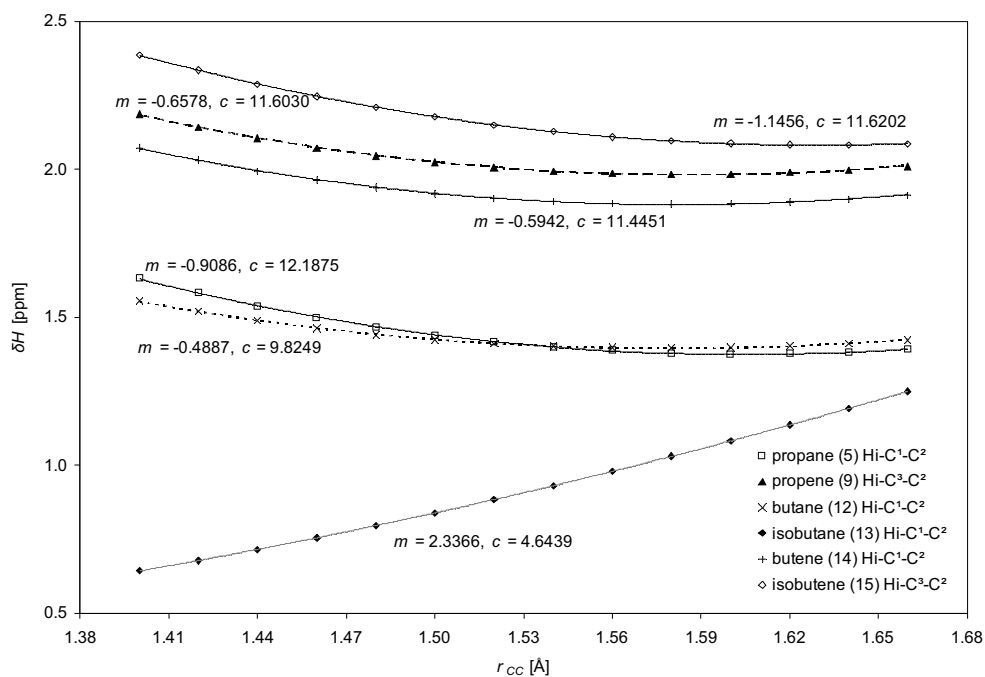
Fig. (6). Examples of ^{1}H shifts of hydrogen bonded to sp^3 hybridized carbon of **set B** in dependence of CC single bond distances: in-plane H^i of **5**, **9**, and **12-15**. The {210} regression curves are designated with their curvatures c and slopes m from linear regression.
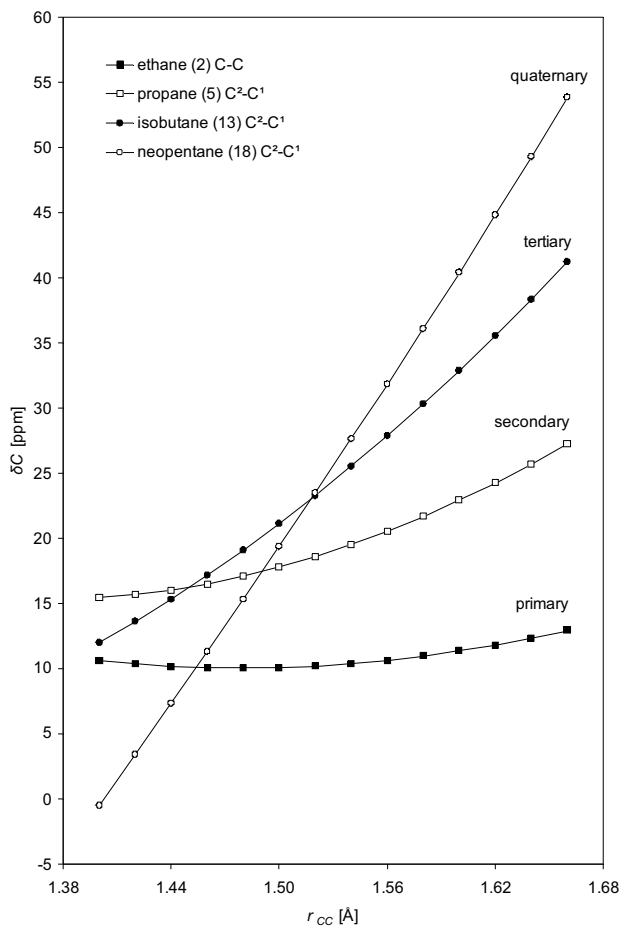
Fig. (7). ^{13}C shifts of sp^3 carbon atoms of **set B** with different coordination in dependence of CC distances.
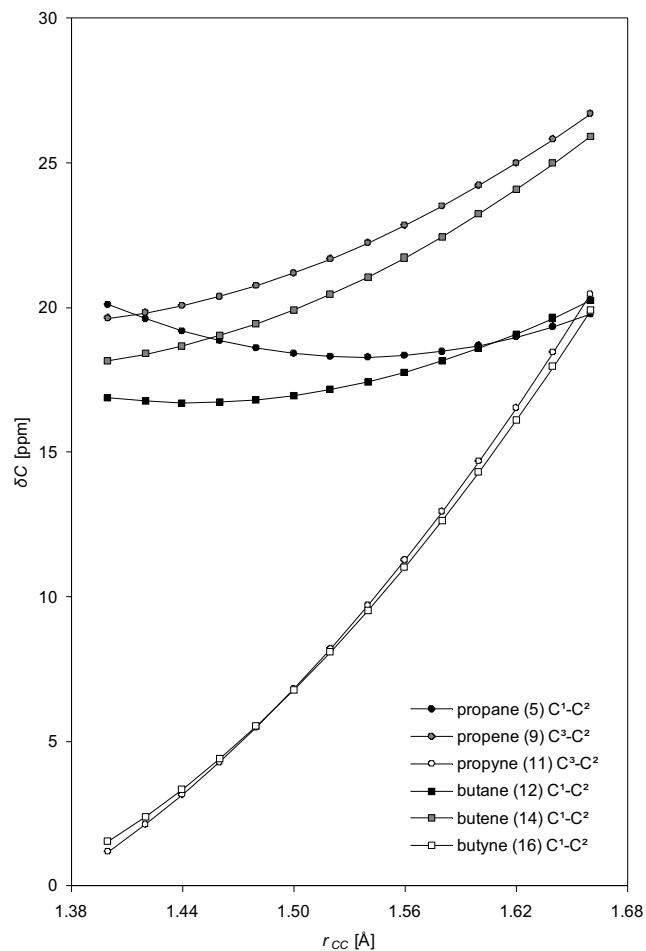
Fig. (8). ^{13}C shifts of primary sp^3 carbon atoms of **set B** bonded to differently hybridized C in dependence of CC distances.

Table 7.   **Linear Slopes (*m*) and Curvatures (*c, derived from {210})* of Graphs of the ¹³C Shifts in Dependence of CC Distances, Sorted by Bond Order (BO), Hybridization (*n_{hyb}*) and Oxidation Number (*n_{ox}*), as Well as Coefficients of Determination (*R^2*) of the Regressions with Different Power Functions. Marking See Text**

No.	Bond	BO	n_{hyb}	n_{ox}	m	c	R^2					
							{10}	{30}	{40}	{50}	{60}	{210}
11	C²-C³	1	1	0	15.91	59.37	0.98244	0.99257	0.99602	0.99839	0.99970	0.99995
16	C²-C¹	1	1	0	17.86	-7.63	0.99976	0.99616	0.99278	0.98839	0.98303	0.99999
17	C²-C³	1	1	0	6.72	107.58	0.75273	0.79620	0.81658	0.83592	0.85414	0.99958
15	C²-C³	1	2	0	43.48	224.12	0.96710	0.98169	0.98737	0.99197	0.99548	1.00000
6	C²-C³	1	2	-1	35.57	76.78	0.99317	0.99904	0.99997	0.99960	0.99797	0.99999
9	C²-C³	1	2	-1	11.01	151.75	0.80435	0.83998	0.85654	0.87218	0.88685	0.99997
14	C²-C¹	1	2	-1	22.14	105.63	0.97166	0.98505	0.99012	0.99408	0.99696	0.99997
18	C²-C¹	1	3	0	208.55	134.25	0.99946	0.99944	0.99782	0.99515	0.99149	0.99999
13	C²-C¹	1	3	-1	112.35	262.09	0.99308	0.99866	0.99981	0.99989	0.99893	1.00000
5	C²-C¹	1	3	-2	45.61	272.30	0.95636	0.97340	0.98031	0.98613	0.99086	0.99998
8	C-C	1	3	-2	60.98	177.34	0.98928	0.99674	0.99883	0.99983	0.99977	0.99999
12	C²-C¹	1	3	-2	2.44	288.93	0.05251	0.07521	0.08781	0.10114	0.11511	0.99864
12	C²-C³	1	3	-2	22.34	155.59	0.94150	0.96143	0.96981	0.97710	0.98330	0.99996
2	C-C	1	3	-3	9.02	176.45	0.67121	0.71420	0.73481	0.75469	0.77379	0.99977
5	C¹-C²	1	3	-3	-1.22	194.68	0.02993	0.01610	0.01080	0.00658	0.00343	0.99998
9	C³-C²	1	3	-3	27.30	143.20	0.96596	0.98082	0.98663	0.99134	0.99496	0.99999
11	C³-C²	1	3	-3	74.23	224.05	0.98847	0.99629	0.99856	0.99975	0.99987	1.00000
12	C¹-C²	1	3	-3	13.11	149.01	0.85808	0.88902	0.90308	0.91615	0.92817	0.99991
13	C¹-C²	1	3	-3	-7.07	224.18	0.43732	0.39137	0.36893	0.34698	0.32559	1.00000
14	C¹-C²	1	3	-3	29.92	154.38	0.96704	0.98164	0.98731	0.99189	0.99539	0.99999
15	C³-C²	1	3	-3	26.28	179.02	0.94392	0.96342	0.97160	0.97869	0.98469	1.00000
16	C¹-C²	1	3	-3	70.74	227.02	0.98698	0.99542	0.99800	0.99949	0.99991	0.99999

(Table 7). Contd…..

No.	Bond	BO	n_{hyb}	n_{ox}	m	c	R^2 {10}	{30}	{40}	{50}	{60}	{210}
18	C^1-C^2	1	3	-3	-12.38	286.46	0.59338	0.54722	0.52418	0.50132	0.47872	0.99989
7	C-C	1.5	2	-1	229.43	807.46	0.98435	0.99451	0.99763	0.99945	1.00000	0.99995
10	C^2-C^1	2	1	0	420.90	1415.19	0.98567	0.99559	0.99840	0.99981	0.99985	0.99993
15	C^2-C^1	2	2	0	226.01	471.08	0.99445	0.99955	0.99996	0.99898	0.99666	0.99998
6	C^2-C^1	2	2	-1	161.61	424.79	0.99123	0.99839	0.99981	0.99982	0.99846	1.00000
9	C^2-C^1	2	2	-1	205.54	488.39	0.99279	0.99901	0.99997	0.99954	0.99776	0.99997
14	C^2-C^3	2	2	-1	188.15	456.63	0.99248	0.99889	0.99995	0.99961	0.99792	0.99997
3	C-C	2	2	-2	182.42	497.77	0.99052	0.99806	0.99969	0.99992	0.99879	0.99996
6	C^1-C^2	2	2	-2	147.06	331.25	0.99354	0.99928	1.00000	0.99932	0.99730	0.99999
9	C^1-C^2	2	2	-2	164.86	459.06	0.99013	0.99788	0.99962	0.99995	0.99892	0.99995
10	C^1-C^2	2	2	-2	181.71	537.19	0.98890	0.99730	0.99935	1.00000	0.99928	0.99996
15	C^1-C^2	2	2	-2	148.11	427.65	0.98940	0.99754	0.99946	0.99999	0.99915	0.99995
11	C^2-C^1	3	1	0	92.88	256.66	0.98886	0.99822	0.99984	0.99948	0.99723	0.99999
16	C^2-C^3	3	1	0	108.24	403.84	0.97982	0.99378	0.99774	0.99973	0.99980	0.99992
17	C^2-C^1	3	1	0	96.88	324.44	0.98373	0.99588	0.99892	0.99998	0.99913	0.99999
4	C-C	3	1	-1	102.85	428.18	0.97499	0.99096	0.99593	0.99892	0.99999	0.99989
11	C^1-C^2	3	1	-1	118.53	578.57	0.96571	0.98497	0.99163	0.99632	0.99909	0.99961
17	C^1-C^2	3	1	-1	75.04	289.41	0.97853	0.99306	0.99730	0.99954	0.99986	0.99997

Fig. (**8**) presents for **set B** a comparison of the non-linear shifts of terminal sp^3 carbon atoms bound to sp^3, sp^2 and sp carbon atoms. Whereas shifts of methyl carbons adjacent to saturated CC bonds in propane (**5**) and butane (**12**) behave different with small slopes and strong curvature, the methyl carbon shifts of alkenes **9** and **14** show close similarities with larger slopes and smaller curvature, and those bonded to triple bonds in **11** and **16** show nearly identical very steep non-linear curves.

The results of polynomial adjustment of the kind of eqn. 3, but now up to an order of six without lower order terms, designated as {30} to {60}, for shifts of all carbons of the molecules of **set B** are presented in Table 7. For sp^2 carbons (BO = 2), the simple polynomial {40} is very often successful, as found before in the case of ^{1}H shifts in Table **6**. This is highlighted gray in Table **7**, where {40} represents a good fit (R^2 larger than 0.999) with exception of **10**. Some cases where the lower polynomial {30} already delivers a good R^2 are printed bold. Similar characterizations are given for {60} and {50} in the case of triple bonded carbons (BO = 3), where the polynomial {60} is a good representation, with the exception of **11**. {210} is useful in all cases of single bonds (BO = 1) and often for other molecules. Linearities are only found for the signals of quaternary C^2 carbons in **16** and **18**.

Simultaneous Variations of CH and CC Bond Lengths

In few cases, we studied the effect of simultaneous variations of CH and CC bond distances on calculated ^{1}H and ^{13}C NMR shifts. The three-dimensional plot for ethene (**3**) from HF/6-311G* calculations (**set B**) in Fig. (**9**) shows an interdependence of the ^{1}H shifts on the two varied distance parameters. The slopes of the approximately linear r_{CH} curves decrease with increasing CC distances. The r_{CC} curve is bent and is steeper for small CH distances (*c* is larger). The graph is saddle-shaped with a convex curvature in the r_{CC} dimension and a concave curvature in the r_{CH} dimension.
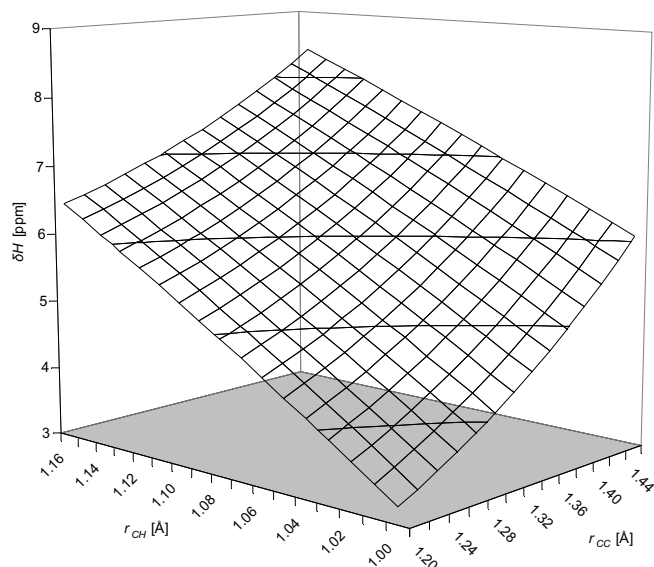
Fig. (9). [1]H shifts of ethene (**3**) from **set B** in dependence of simultaneous CC and CH bond distance variations.

The surface of ^{13}C shifts presented in Fig. (**10**) is less curved than that of Fig. (**9**). It shows non-linearities in both distance dimensions. The convex curvature for the r_{CH} variation is strongly increasing with enlargement of CC distances, but slopes for one kind of distance variation are independent on variation of the other one. Characteristic numerical data for both shift ranges of **3** are collected in Table **8**.
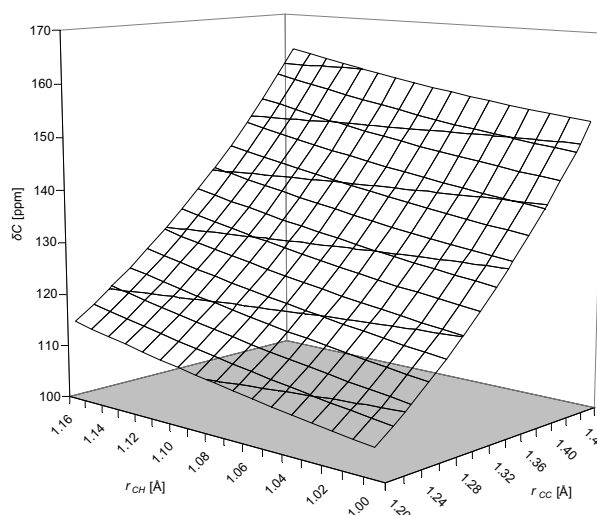
Fig. (10). [13]C shifts of ethene (**3**) from **set B** in dependence of simultaneous CC and CH bond distance variations.

Angular Variations

The influence of symmetric variations of angles on ^{1}H and ^{13}C shifts was studied under conditions of **set A** for the CCH angles of ethane (**2**) and of ethene (**3**) in steps of 0.5° for a range of ± 5° around the experimental angle. As an example of the CCC angle variation, propane (**5**) was chosen. A range of ± 10° around the experimental CCC angle was scanned in steps of 1°. The results are presented solely graphically.

Fig. (**11**) shows the change of ^{1}H and ^{13}C shifts for **3** in dependence on the CCH angle. Increase of the angle leads to a decrease of both types of chemical shifts. The dependence is rather small with values of -0.09 ppm/1° for ^{1}H and -1.4 ppm/1° for [13]C. The angular ^{13}C dependence of **3** is nearly linear with $R^2 = 0.9984$. For **2**, similar, non-linear behavior was observed. Equations for quadratic {210} approximations are included in the graphs.

The influence of angular CCC variations on three proton shifts and two carbon shifts of **5** is depicted in Fig. (**12**). The

Table 8.   **Slopes (m), Coefficients of Determination (R^2_{lin}) and Curvatures (c) of the Boundary Curves of the ^{1}H and [13]C Shift Surfaces of Ethene (3) from Set B**

		Variation of r_{CH}		Variation of r_{CC}	
		min. r_{CC}	max. r_{CC}	min. r_{CH}	max. r_{CH}
[1]H shift [a]	m	20.18	14.52	10.82	7.34
	R^2_{lin}	0.9992	0.9997	0.9894	0.9867
	c	-26.96	-12.28	31.28	23.79
[13]C shift [b]	m	59.55	58.47	183.79	183.12
	R^2_{lin}	0.9955	0.9901	0.9906	0.9906
	c	183.8	268.19	499.08	497.89

[a]See Figure 9. [b] See Figure 10.
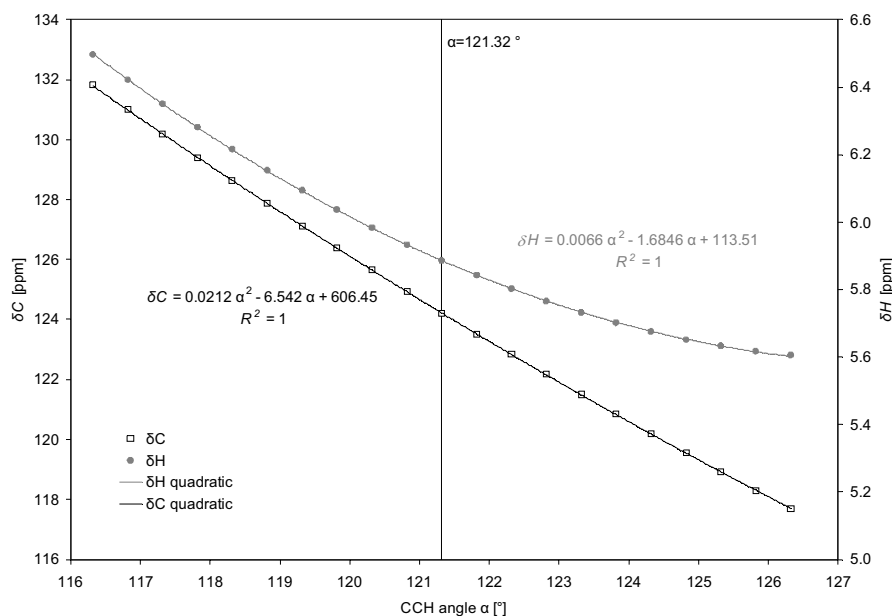
Fig. (11). Dependence of ^{1}H and ^{13}C chemical shifts of **3 (set A)** of the CCH angle. Best fit curves are given as well as equations and coefficients of determination.

proton signals in-plane δH^i and out-of-plane δH^o show convex and rather flat curves with slopes of -0.004 and 0.003 ppm/1° which can be approximated by quadratic {210} polynomials. However, the methylene δH^2 signal is more strongly curved with about -0.024 ppm/1° and can only be approximated by a third order polynomial. The same refers to ^{13}C NMR for the δC^2 signals with -0.21 ppm/1°, whereas the δC^1 curve is only slightly convex and rather steep with -0.34 ppm/1°.

The effect of CCC angle variation in **5** is less than that of CCH variation in **2** and **3**. In all but one case (δH^o), a decrease of shifts with increase of angles is observed.

Relation of Geometric Variations of Chemical Shift to Amplitudes of Vibration

Values of total energies are derived from each step of the distance variation. These can be used to determine an anharmonic energy curve which can be very well approximated
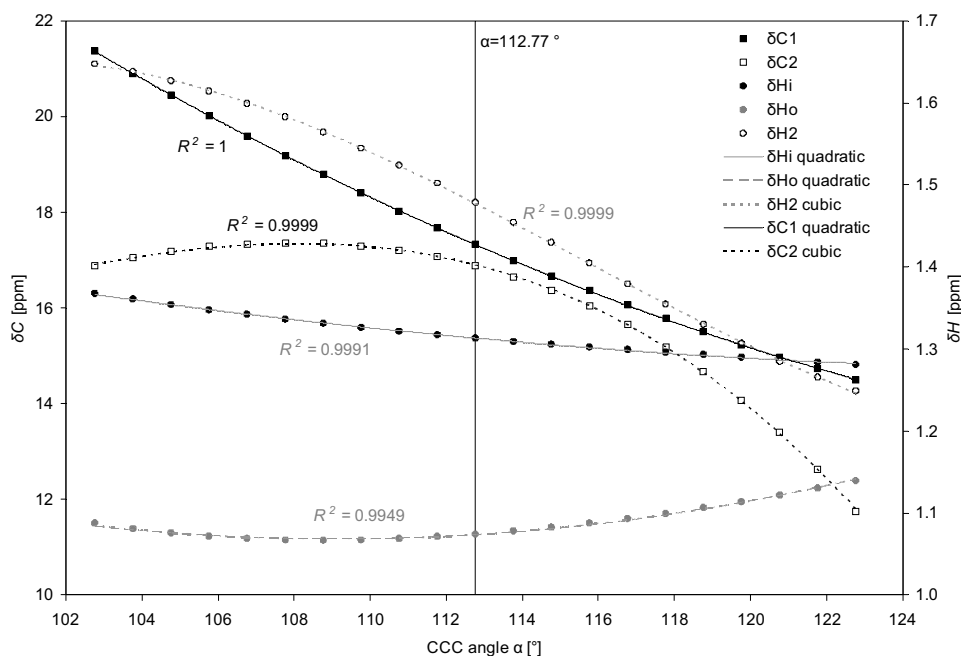
Fig. (12). Dependence of ^{1}H and ^{13}C chemical shifts of **5 (set A)** of the CCC angle. Only the coefficients of determination of the best fit curves are given. The order of the fitting polynomial is indicated next to the lines in the legend.
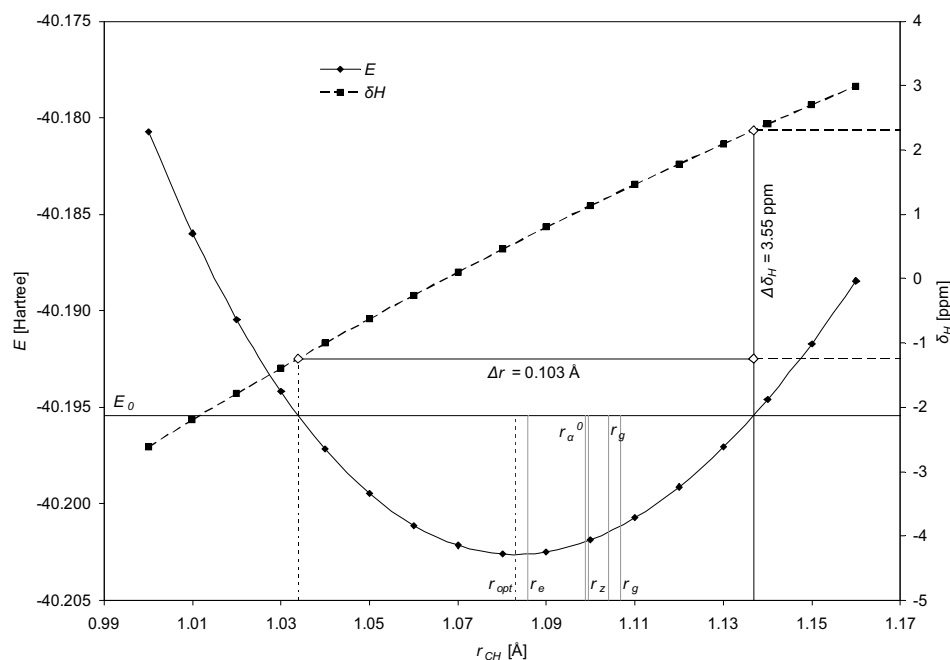
Fig. (13). Total energy (left scale) and proton chemical shift (right scale) of methane (**1**) in dependence of CH distance (HF/6-311G* calculations). Distance and shift intervals Δr and $\Delta \delta$ for the symmetric CH stretching vibration are highlighted. Additionally depicted are the zero-point energy level E_0, the optimized CH distance r_{opt} as well as some experimental distances (r_e, r_α^0, r_z and r_g).

by a third order polynomial with the result shown in Fig. (**13**) for the HF/6-311G* calculation of methane (**1**). An additional frequency calculation for the minimum geometry (r_{opt}) leads to a value for the lowest totally symmetric zero-point vibrational energy level (E_0) which is drawn as a horizontal line in Fig. (**13**). This line determines a range of 0.103 Å as a possible vibrational amplitude which corresponds to a hypothetical range of 3.55 ppm for the derived variation of

the ^{1}H chemical shift of **1**. But only one single shift value is observed experimentally. Therefore the total vibrational amplitude is irrelevant for the explanation of the experimentally observed chemical shift. Contrary to the classical picture for harmonic vibrations, the probabilities of positions at end points are not important. Instead of this, quantum chemical locations of the zero-point vibrational state are most probable at the calculated center (r_{opt}), the minimum of the
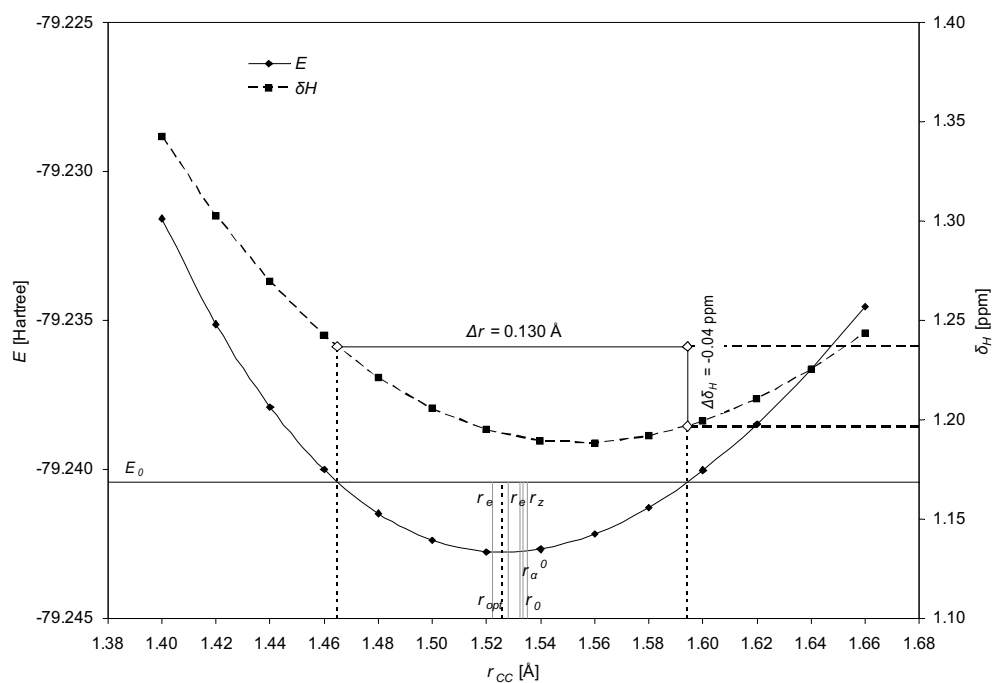
Fig. (14). Total energy and proton chemical shift of ethane (**2**) in dependence of CC distance. Distance and shift intervals for symmetric CC stretching vibration are included. Scales and details as those used in Fig. (**13**).

Table 9.   Zero-Point Vibrational Corrections ($\Delta\delta$) for ^{1}H and ^{13}C Chemical Shifts. Experimental Distances in Å

			No.	1	2	3	4	7
				Methane	Ethane	Ethene	Ethyne	Benzene
CH variation	CH distances	r_e		1.086 [a]	1.089 [b]	1.081 [c]	1.062 [d]	1.080 [e]
		r_z		1.100 [f]	1.102 [g]	1.087 [h]		1.083 [i]
		r_z - r_e		0.013	0.013	0.006		0.003
		r_g		1.104 [j]	1.112 [k]	1.103 [h]	1.078 [l]	1.101 [i]
		r_g - r_e		0.018	0.023	0.022	0.016	0.021
	^{1}H	m	6-31G*	33.702	33.084	17.206	31.777	13.387
			6-311G*	34.972	34.537	17.703	32.313	13.303
		$\Delta\delta\, r_z$	6-31G*	0.448	0.420	0.103		0.037
			6-311G*	0.465	0.439	0.106		0.037
		$\Delta\delta\, r_g$	6-31G*	0.600	0.768	0.380	0.506	0.278
			6-311G*	0.623	0.801	0.391	0.514	0.277
		$\Delta\delta_{ZPV}$	Ref. [m]	0.59	0.67	0.52	0.76	0.38
	^{13}C	m	6-31G*	201.527	203.442	57.725	6.134	36.776
			6-311G*	201.089	213.224	59.058	2.859	39.263
		$\Delta\delta\, r_z$	6-31G*	2.680	2.584	0.346		0.103
			6-311G*	2.674	2.708	0.354		0.110
		$\Delta\delta\, r_g$	6-31G*	3.587	4.720	1.276	0.098	0.765
			6-311G*	3.579	4.947	1.305	0.046	0.817
		$\Delta\delta_{ZPV}$	Ref. [m]	3.20	3.95	4.79	4.44	3.37
CC variation	CC distances	r_e			1.522 [b]	1.331 [c]	1.203 [d]	1.391 [e]
		r_z			1.535 [n]	1.339 [h]		1.397 [i]
		r_z - r_e			0.013	0.008		0.005
		r_g			1.534 [k]	1.337 [p]	1.212 [l]	1.399 [i]
		r_g - r_e			0.012	0.006	0.009	0.008
	^{1}H	m	6-31G*		-0.185	8.881	5.193	11.992
			6-311G*		-0.348	8.896	5.973	12.132
		$\Delta\delta\, r_z$	6-31G*		-0.002	0.075		0.064
			6-311G*		-0.005	0.075		0.064
		$\Delta\delta\, r_g$	6-31G*		-0.002	0.055	0.048	0.094
			6-311G*		-0.004	0.055	0.055	0.095
		$\Delta\delta_{ZPV}$	Ref. [m]	0.59	0.67	0.52	0.76	0.38
		$\Sigma\Delta\delta\, r_z$	6-311G*	0.47	0.43	0.18		0.10
		$\Sigma\Delta\delta\, r_g$	6-311G*	0.62	0.80	0.45	0.57	0.37
	^{13}C	m	6-31G*		16.768	188.632	113.463	232.694
			6-311G*		9.023	182.419	102.850	229.430
		$\Delta\delta\, r_z$	6-31G*		0.220	1.585		1.233
			6-311G*		0.118	1.532		1.216
		$\Delta\delta\, r_g$	6-31G*		0.201	1.170	1.053	1.815
			6-311G*		0.108	1.131	0.954	1.790
		$\Delta\delta_{ZPV}$	Ref. [m]	3.20	3.95	4.79	4.44	3.37
		$\Sigma\Delta\delta\, r_z$	6-311G*	2.67	2.83	1.89		1.33
		$\Sigma\Delta\delta\, r_g$	6-311G*	3.58	5.06	2.44	1.00	2.61

References: [a] [54]; [b] [55]; [c] [56]; [d] [57]; [e] [58]; [f] [59]; [g] [60]; [h] [61]; [i] [62]; [j] [63]; [k] [64]; [l] [65]; [m] [33]; [n] [66]; [o] [67]; [p] [68].

energy curve, which is close but not identical to the experimental r_e value. Because of the anharmonicity of the energy curve, comparison of experimental shifts with calculations has to be done using vibrationally averaged structures and corresponding chemical shifts. This was suggested as vibrational mode following by Dransfeld [49] or as vibrational corrections to the shieldings in the groups of Raynes [31] for ^{13}C of **1**, Ruud [33] for ^{1}H and ^{13}C, and Auer [50] for ^{13}C,

which usually lead to a numerical increase of calculated shifts (or lowering of shieldings).

In Fig. (**13**) are marked experimental microwave (MW) r_z and electron diffraction (ED) r_a^0 CH distances of **1** which refer physically to experimental bond lengths at the zero-point vibrational level at 0 K. In contrast to this, experimental ED r_g values correspond to a thermally averaged molecular structure [51], for which two independent different experimental determinations for **1** are available. These distances are all larger than the equilibrium structure (r_e) and might better be taken as useful geometries for approximative calculations of chemical shifts. Such a distance change from $r_e = 1.086(1)$ Å to $r_z = 1.099(1)$ Å would lead from the graph of shift variations to an increase of ^{1}H shifts by 0.45 ppm. Unfortunately, this correction in the HF/6-311G* calculations of **1** leads from the r_e based chemical shift of 0.667 ppm to 1.117 ppm for r_z. However, both values are far from the experimental gas phase value of 0.14 ppm. This is due to deficiencies of the HF model calculation, the applied basis set and the TMS calculation. Better agreement to the experiment needs at least use of the MP2 model in combination with calculations using consecutive Dunning correlation consistent basis sets and extrapolation to the basis set limit [52] or advanced post-HF methods with large basis sets, see the review on benchmark calculations by Gauss and Stanton [2]. Accurate CCSD(T) calculations of shieldings of **1** are presented by Gauss *et al.* [29,50] and MC-SCF calculations by Ruud *et al.* [30]. A complete basis set DFT study was reported by Kupka *et al.* [53].

Fig. (**14**) shows a similar plot of total energies in dependence of the variation of CC distances of ethane (**2**). This leads to an overall zero-point vibrational amplitude (Δr) of 0.13 Å. The corresponding behavior of the proton chemical shift (δ_H) on CC variation which shows now a non-linear

curved dependence is also inserted in the graph. The total amplitude covers a shift range ($\Delta\delta_H$) of 0.04 ppm. Experimental CC distances increase from $r_e = 1.528(3)$ Å to 1.532(2) Å for r_z. This leads here to a small decrease of the chemical shift by -0.004 ppm. The similar CH vibrational correction for **2** amounts to a larger value of 0.439 ppm (see Table **9**). Both corrections increase the calculated chemical shift from 1.151 ppm for r_e geometry to 1.596 ppm and increase the deviation from the experimental shift which is with 0.88 ppm again at higher field.

^{13}C chemical shifts are considered in the following two figures for ethane (**2**). The energy dependence on CH distance variations in Fig. (**15**) shows a total zero-point vibrational amplitude of 0.085 Å. Its relation to the linear ^{13}C shift variation curve leads to a large change ($\Delta\delta_C$) of 18.18 ppm. Again only the increase of CH distances from $r_e = 1.088(3)$ Å to $r_z = 1.102(2)$ Å may be considered as relevant, leading to a shift correction by 2.71 ppm from 9.813 ppm to 12.523 ppm, but the experimental gas phase ^{13}C shift is 7.2 ppm.

The dependence of the total energy and the ^{13}C shift of **2** on CC distance variation is shown in Fig. (**16**). The over all zero-point vibrational amplitude Δr amounts to 0.13 Å and the corresponding non-linear shift curve shows a corresponding ^{13}C shift change of 1.19 ppm. The smaller distance elongation from $r_e = 1.528(3)$ Å to $r_z = 1.532(2)$ Å corresponds to an additional shift increase of 0.12 ppm increasing the above mentioned shift to 12.643 ppm in relation to the experimental shift value of 7.2 ppm.

Estimation of Vibrational Corrections for ^{1}H and ^{13}C Chemical Shifts

The above mentioned zero-point vibrational corrections do not lead to an improvement of HF calculations in relation to experimental chemical shifts, however they allow a simple
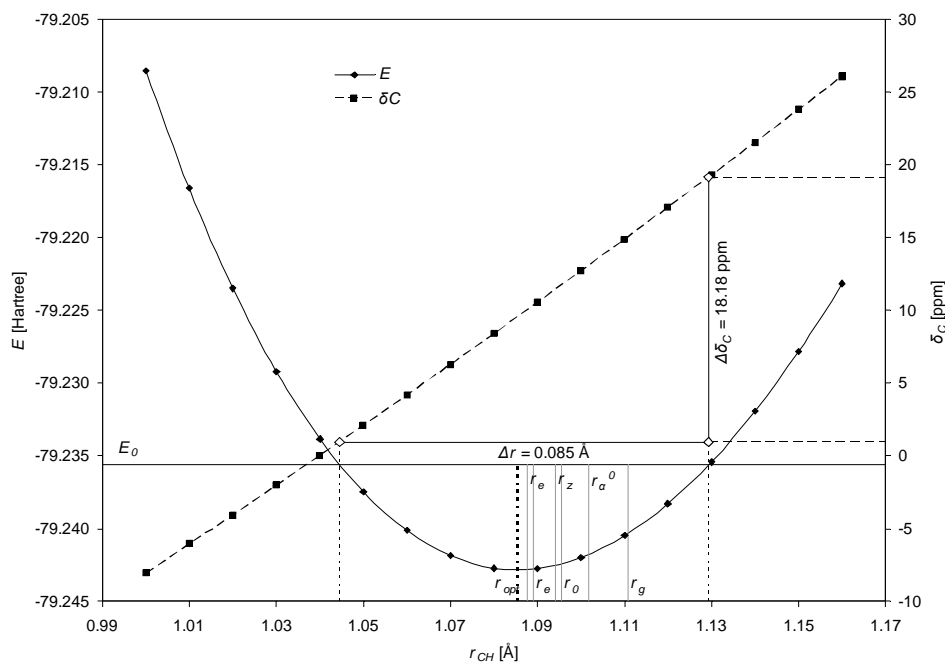
Fig. (15). Total energy and carbon chemical shift of ethane (**2**) in dependence of CH distance. Distance and shift intervals for the lowest symmetric CH stretching vibration are included as in Fig. (**13**).
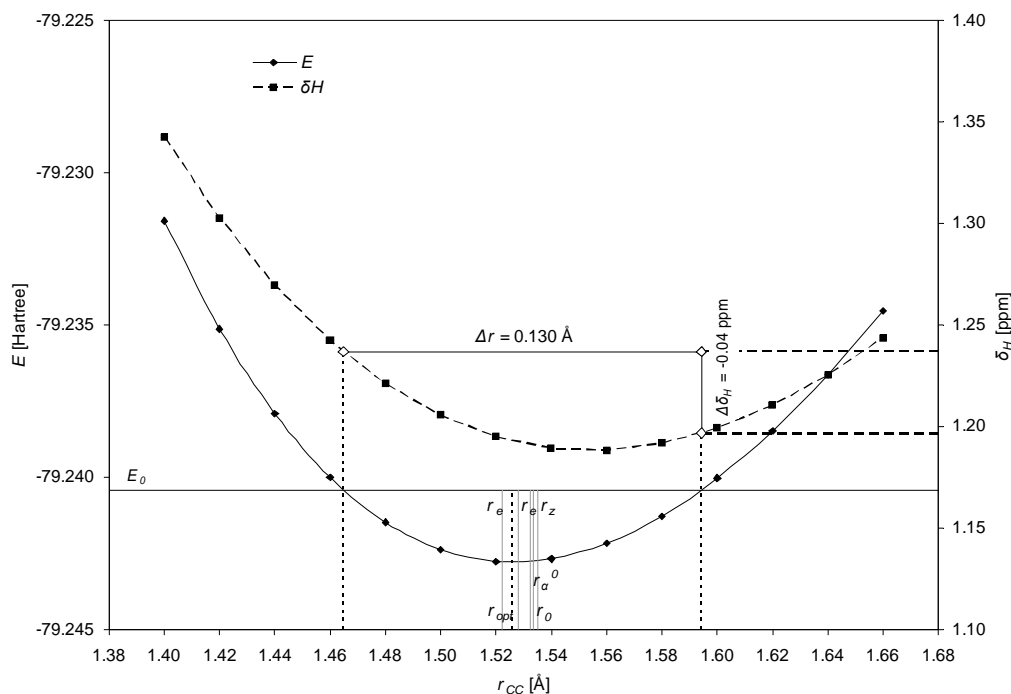
Fig. (16). Total energy and carbon chemical shift of ethane (**2**) in dependence of CC distance. Distance and shift intervals for the symmetric CC stretching vibration are included as in Fig. (**13**).

estimation of the size of this ZPV correction for shift or shielding calculations by use of eqn. 4.

$$\Delta\delta_{ZPV} \text{ [ppm]} = m \cdot \Delta r \qquad (4)$$

The slopes (m) of linear regressions listed in Tables **3** and **6** for ^{1}H shifts and 4, 5, 7 for ^{13}C shifts are multiplied by the difference ($\Delta r = r_z - r_e$) between r_e (the experimental distance at the minimum of the energy curve) and r_z (the experimental bond length for the zero-point vibrational level) or r_g (the experimental ED distance for a thermal average of rotational and vibrational states). This leads to an estimation of ZPV shift or shielding corrections. Absolute shielding corrections ($\Delta\sigma_{ZPV}$) have a negative sign and chemical shift corrections ($\Delta\delta_{ZPV}$) based on the TMS scale have a positive sign, both indicating a low field shift due to reduced shielding.

Corresponding values for 6-31G* (**set A**) and 6-311G* (**set B**) calculations for few molecules with known experimental r_e distances related to known experimental r_z and r_g distances are collected in Table **9** in comparison to ZPV values from reference [33].

Our estimations for ^{1}H shift corrections show a small basis set dependence; therefore we concentrate our discussion on the 6-311G* calculations from **set B**. For methane (**1**), whose shift depends only on CH distances, our smaller r_z and the larger r_g corrections are bracketing the ZPV values from the literature for both ^{1}H and ^{13}C shifts. For other molecules, the estimated CH and CC corrections have to be added to give $\Sigma\Delta\delta$ which are indicated and compared to the literature results in Table **9**. As expectable for ^{1}H shift corrections, the effect of CH distance variation is larger than that of the CC variation, which shows in the case of ethane (**2**) even a small negative value. For **2**, the r_z and r_g derived corrections are also bracketing the literature value of 0.67 ppm. For **3** and **4**, our estimations lead to smaller values than the published

corrections. In the case of **7**, the r_g correction is close to the published value, however, the r_z based values are much too low.

The ^{13}C shift ZPV corrections are in a range of 1.0 to 5.0 ppm. For **2**, the value of the CH variation is larger than that of the CC variation which is reversed for the other molecules. Our predicted $\Delta\delta_{ZPV}$ correction is larger than the reference value for **2** but smaller for the other three examples.

Our simple procedure by use of eqn. 4 leads to predictions of ZPV corrections for ^{1}H shifts with deviation up to 0.2 ppm and for ^{13}C shifts up to 3 ppm. As experimental r_e values are only rarely available, they may be replaced by distances determined from complete basis set extrapolations [48,52]. The experimental r_z and r_g bond lengths may be replaced by HF/6-311G* optimized distances.

CONCLUSIONS

Stepwise variations of CH or CC bond distances related to HF GIAO calculations of ^{1}H and ^{13}C chemical shifts in 6-31G* (**set A**) and 6-311G* (**set B**) basis sets of 18 different hydrocarbons lead to smooth curves for each molecule. Generally with few exceptions, an increase of distances leads to low field shifts. For ^{1}H shifts the dependences on CH distances are mostly linear or slightly curved (see Tables **3** and **4** and Figure). The slopes of linear least squares regressions may be grouped according to hybridization and substitution pattern as shown in Fig. (**3**). The dependence of ^{13}C chemical shifts on CH distances is also nearly linear for saturated and olefinic hydrocarbons, but curved for triple bonded CH as shown in Fig. (**4**). CC distance variations lead to curved dependencies for ^{1}H shifts (Figs. **5** and **6**) as well as for ^{13}C shifts (Fig. **8**). These may be approximated by different polynomial regressions as collected in Tables **5** and **6**. Simultaneous variations of CH and CC distances for three ex-

amples show a small interdependence of the two dimensions for both ^{1}H and ^{13}C chemical shifts (see Figs. **9** and **10**). Variations of CCH and CCC angles of three molecules show a decrease of ^{1}H and ^{13}C shifts with increase of angles (see Figs. **11** and **12**). For methane (**1**) and ethane (**2**), the distance dependence of total energies was plotted in (Figs. **13** to **16**). The resulting graph of corresponding zero-point energy levels leads to an estimation of the size of the vibrational amplitude of the molecules in motion at room temperature, but the corresponding geometry dependent experimental chemical shift is independent on this large amplitude of vibration. The slopes of derived linear regressions may be used to estimate zero-point vibrational corrections to chemical shifts *via* eqn. 4 as shown in Table **9**.

REFERENCES

[1] Helgaker T, Jaszunski M, Ruud K. Ab initio methods for the calculation of NMR shielding and indirect spin-spin coupling constants. Chem Rev 1999; 99: 293-352.

[2] Gauss J, Stanton JF. Electron-correlated approaches for the calculation of NMR chemical shifts. Adv Chem Phys 2002; 123: 355-422.

[3] Kaupp M, Bühl M, Malkin VG. Calculation of NMR and EPR Parameters, Theory and Applications. Weinheim: Wiley-VCH; 2004.

[4] Ramsay NF. Magnetic shielding of nuclei in molecules. Phys Rev 1950; 78: 699-703.

[5] Kutzelnigg W. Theory of magnetic susceptibilities and NMR chemical shifts in terms of localized quantities. Isr J Chem 1980; 19: 193-200.

[6] Schindler M, Kutzelnigg W. Theory of magnetic susceptibilities and NMR chemical shifts in terms of localized quantities. II. Application to some simple molecules. J Chem Phys 1982; 76: 1919-33.

[7] Hansen AE, Bouman TD. Localized orbital/local origin method for calculation and analysis of NMR shieldings. Applications to 13C shielding tensors. J Chem Phys 1985; 82: 5035-47.

[8] Keith TA, Bader RF. Calculation of magnetic response properties using a continuous set of gauge transformations. Chem Phys Lett 1993; 210: 223-31.

[9] London F. Théorie quantique des courants interatomiques dans les combinaisons aromatiques. J Phys Radium 1937; 8: 397-409.

[10] Ditchfield R. On molecular orbital theories of NMR chemical shifts. Chem Phys Lett 1972; 15: 203-6.

[11] Ditchfield R. Self-consistent perturbation theory of diamagnetism. I. A gauge-invariant LCAO method for N.M.R. chemical shifts. Mol Phys 1974; 27: 789-807.

[12] Wolinski K, Hinton JF, Pulay P. Efficient implementation of the gauge-independent atomic orbital method fro NMR chemical shift calculations. J Am Chem Soc 1990; 112: 8251-60.

[13] Frisch MJ, Trucks GW, Schlegel HB, *et al.* Gaussian 98. Revision A.7. Pittsburgh PA: Gaussian, Inc.; 1998.

[14] Frisch MJ, Trucks GW, Schlegel HB, *et al.* Gaussian 03. Revision C.02. Wallingford CT: Gaussian, Inc.; 2004.

[15] Chesnut DB, Foley CK. Chemical shifts and bond modification effects for some small first-row-atom molecules. J Chem Phys 1986; 84: 852-61.

[16] Chesnut DB, Phung CG. Nuclear magnetic resonance chemical shifts using optimized geometries. J Chem Phys 1989; 91: 6238-45.

[17] Chesnut DB, Wright DW. Chemical shift bond derivatives for molecules containing first-row atoms. J Comput Chem 1991; 12: 546-59.

[18] McMichael Rohlfing C, Allen LC, Ditchfield R. Proton and carbon-13 chemical shifts: comparison between theory and experiment. Chem Phys 1984; 87: 9-15.

[19] Fukui H, Baba T, Matsuda H, Miura K. Calculation of nuclear magnetic shieldings. IX. Electron correlation effects. J Chem Phys 1994; 100: 6608-13.

[20] Cheeseman JR, Trucks GW, Keith TA, Frisch MJ. A comparison of models for calculating nuclear magnetic resonance shielding tensors. J Chem Phys 1996; 104: 5497-509.

[21] Chesnut DB. On the calculation of hydrogen NMR chemical shielding. Chem Phys 1997; 214: 73-9.

[22] Hehre WJ, Radom L, von Ragué Schleyer P, Pople J. Ab Initio Molecular Orbital Theory. New York: Wiley-Interscience; 1986.

[23] Koch W, Holthausen MC. A Chemists Guide to Density Functional Theory. Weinheim: Wiley-VCH; 1999.

[24] Møller C, Plesset MS. Note on an approximation treatment for many-electron systems. Phys Rev 1934; 46: 618-22.

[25] Gauss J. Effects of electron correlation in the calculation of nuclear magnetic resonance chemical shifts. J Chem Phys 1993; 99: 3629-43.

[26] Gauss J. GIAO-MBPT(3) and GIAO-SDQ-MBPT(4) calculations of nuclear magnetic shielding constants. Chem Phys Lett 1994; 229: 198.

[27] Gauss J, Stanton JF. Gauge-invariant calculation of nuclear magnetic shielding constants at the coupled-cluster singles and doubles level. J Chem Phys 1995; 102: 251-3.

[28] Gauss J, Stanton JF. Coupled-cluster calculations of nuclear magnetic resonance chemical shifts. J Chem Phys 1995; 103: 3561-77.

[29] Gauss J, Stanton JF. Perturbative treatment of triple excitations in coupled-cluster calculations of nuclear magnetic shielding constants. J Chem Phys 1996; 104: 2574.

[30] Ruud K, Helgaker T, Kobayashi R, Jørgensen P, Bak KL, Jensen HJ. Multiconfigurational self-consistent field calculation of nuclear shieldings using London atomic orbitals. J Chem Phys 1994; 100: 8178-85.

[31] Raynes WT, Fowler PW, Lazzeretti P, Zanasi R, Grayson M. The effects of rotation and vibration on the carbon-13 shielding, magnetizabilities and geometrical parameters of some methane isotopomers. Mol Phys 1988; 64: 143-62.

[32] Sundholm D, Gauss J, Schäfer A. Rovibrationally averaged nuclear magnetic shielding tensors calculated at the coupled-cluster level. J Chem Phys 1996; 105: 11051-9.

[33] Ruud K, Åstrand PO, Taylor PR. An efficient approach for calculating vibrational wave functions and zero-point vibrational corrections to molecular properties of polyatomic molecules. J Chem Phys 2000; 112: 2668-83.

[34] Ruud K, Åstrand PO, Taylor PR. Zero-point vibrational effects on proton shieldings: functional-group contributions from ab initio calculations. J Am Chem Soc 2001; 123: 4826-33.

[35] Vaara J, Ruud K, Vahtras O. Second- and third-order spin-orbit contributions to nuclear shielding tensors. J Chem Phys 1999; 111: 2900-9.

[36] Cammi R, Mennucci B, Tomasi J. Nuclear magnetic shieldings in solution: Gauge invariant atomic orbital calculation using the polarizable continuum model. J Chem Phys 1999; 110: 7627-38.

[37] Jackowski K, Raynes WT. Density-dependent magnetic shielding in gas phase 13C NMR. Mol Phys 1977; 34: 465-75.

[38] Jameson AK, Jameson CJ. Gas-phase 13C chemical shifts in the zero-pressure limit: refinements to the absolute shielding scale for 13C. Chem Phys Lett 1987; 134: 461-6.

[39] Campanelli AR, Ramondo F, Domenicano A, Hargittai I. Toward a more accurate silicon stereochemistry: an electron diffraction study of the molecular structure of tetramethylsilane. Struct Chem 2000; 11: 155-9.

[40] Alkorta I, Elguero J. Ab initio hybrid DFT-GIAO calculations of the shielding produced by carbon-carbon bonds and aromatic rings in 1H NMR spectroscopy. New J Chem 1998: 381-5.

[41] Rablen PR, Pearlman SA, Finkbiner J. A Comparison of density functional methods for the estimation of proton chemical shifts with chemical accuracy. J Phys Chem A 1999; 103: 7357-63.

[42] Wang B, Fleischer U, Hinton JF, Pulay P. Accurate prediction of proton chemical shifts. I. substituted aromatic hydrocarbons. J Comput Chem 2001; 22: 1887-95.

[43] Gauss J. Analytic second derivatives for the full coupled-cluster singles, doubles, and triples model: Nuclear magnetic shielding constants for BH, HF, CO, N2, N2O, and O3. J Chem Phys 2002; 116: 4773-6.

[44] Zuschneid T, Fischer H, Handel T, Albert K, Häfelinger G. Experimental gas phase 1H NMR Spectra and basis set dependence of ab initio GIAO MO calculations of 1H and 13C NMR absolute shieldings and chemical shifts of small hydrocarbons. Z Naturforsch 2004; 59b: 1153-76.

[45] Becke AD. Density-functional thermochemistry. III. The role of exact exchange. J Chem Phys 1993; 98: 5648-52.

[46] Stephens PJ, Devlin FJ, Chabalowski CF, Frisch MJ. Ab Initio calculation of vibrational absorption and circular dichroism spectra

using density functional force fields. J Phys Chem 1994; 98: 11623-7.

[47]   Dunning TH. Gaussian basis sets for use in correlated molecular calculations. I. The atoms boron through neon and hydrogen. J Chem Phys 1989; 90: 1007-23.

[48]   Neugebauer A, Häfelinger G. Prediction of experimentally unknown re-distances of organic molecules from Dunning basis set extrapolations for ab initio post-HF calculations. J Phys Org Chem 2006; 19: 196-205.

[49]   Dransfeld A. Isotope effects on nuclear magentic shieldings calculated by including zero-point vibration corrections: the VMF approach. Chem Phys 2004; 298: 47-53.

[50]   Auer AA, Gauss J, Stanton JF. Quantitative prediction of gas-phase 13C nuclear magnetic shielding constants. J Chem Phys 2003; 118: 10407-17.

[51]   Vilkov LV, Mastrynkov VS, Sadova NI. Determination of the Geometrical Structure of Free Molecules. Mir Publ., Moscow; 1983.

[52]   Kupka T, Ruscic B, Botto RE. Toward Hartree-fock- and density functional complete basis-set-predicted NMR parameters. J Phys Chem A 2002; 106: 10396-407.

[53]   Kupka T, Ruscic B, Botto RE. Hartree-Fock and density functional complete basis-set (CBS) predicted nuclear shielding anisotropy and shielding tenso components. Solid State Nucl Magn Reson 2003; 23: 145-67.

[54]   Bartell LS, Kuchitsu HK. Representations of molecular force fields. V. On the equilibrium structure of methane. J Chem Phys 1978; 68: 1213-5.

[55]   Harmony MD. The equilibrium carbon–carbon single-bond length in ethane. J Chem Phys 1990; 93: 7522-3.

[56]   Martin JML, Taylor PR. The geometry, vibrational frequencies, and total atomization energy of ethylene. A calibration study. Chem Phys Lett 1996; 248: 336-44.

[57]   Martin JML, Lee TJ, Taylor PR. A purely ab initio spectroscopic quality quartic force field for acetylene. J Chem Phys 1998; 108: 676-91.

[58]   Gauss J, Stanton JF. The equilibrium structure of benzene. J Phys Chem A 2000; 104: 2865-8.

[59]   Morino Y, Kuchitsu K, Oka T. Internuclear distance parameters. J Chem Phys 1962; 36: 1108-9.

[60]   Iijima T. Molecular structure of ethane. Comparison of the structure parameters of CH3CD3 in the torsionally excited state and in the ground state. Bull Chem Soc Jpn 1973; 46: 2311-4.

[61]   Hirota E, Endo Y, Saito S, Yoshida K, Yamaguchi I, Machida K. Microwave spectra of deuterated ethylenes: Dipole moment and rz structure. J Mol Spectr 1981; 89: 223-31.

[62]   Tamagawa K, Iijima T, Kimura M. Molecular structure of benzene. J Mol Struct 1976; 30: 243-53.

[63]   Fink M, Schmiedekamp CW, Gregory D. Precise determination of differential electron scattering cross sections. II. CH4, CO2, CF4. J Chem Phys 1979; 71: 5238-42.

[64]   Bartell LS, Higginbotham HK. Electron diffraction study of the structures of ethane and deuteroethane. J Chem Phys 1965; 42: 851-6.

[65]   Tanimoto M, Kuchitsu K, Morino J. Bond lengths of dimethylacetylene as determined by gas electron diffraction. Bull Chem Soc Jpn 1969; 42: 2519-23.

[66]   Duncan JL, McKean DC, Bruce AJ. Infrared Spectroscopic Studies of Partially Deuterated Ethanes and the r0, rz, and re Structures. J Mol Spectr 1979; 74: 361-74.

[67]   Baldacci A, Ghersetti S, Hurlock SC, Narahari Rao K. Infrared bands of 12C2HD. J Mol Spectr 1976; 59: 116-25.

[68]   Bartell LS, Roth EA, Hollowell CD, Kuchitsu K, Young JE. Electron-diffraction study of the structures of C2H4 and C2D4. J Chem Phys 1965; 42: 2683-6.